Eur. Phys. J. B **12**, 431–449 (1999)

THE EUROPEAN PHYSICAL JOURNAL B

EDP Sciences

Calculation of scattering from stretched copolymers using the tube model: a generalisation of the RPA

D.J. Read[a]

I.R.C. in Polymer Science and Technology, Department of Physics, University of Leeds, Leeds, LS2 9JT, UK

Received 26 October 1998 and Received in final form 19 March 1999

Abstract. There are many experimental situations in which polymer chains are constrained or localised into a small region of space (*e.g.* melt chains confined to a "tube", network chains pinned by crosslinks). We show that detailed consideration of the quenched variables is vital in these experiments. This paper provides a crucial link between microscopic models with localising constraints and scattering patterns by a generalisation of the Random Phase Approximation (RPA) which allows for quenched translational variables. A method is developed which deals with correlations between the quenched variables brought about by incompressiblity (for example, in a polymer melt there are correlations between tubes because of the interaction between chains). As an example, the generalised RPA is applied to models based on the Warner-Edwards picture of the tube. Theoretical results for a melt of H-shaped copolymers are compared with experimental scattering. Early results suggest that to fit the scattering we may be forced to relax one of the central assumptions of the tube model; that the tube deforms affinely, that all chains retract by the same amount or that the tube diameter does not couple to the strain.

PACS. 61.12.Bt Theories of diffraction and scattering – 61.41.+e Polymers, elastomers, and plastics – 83.10.Nn Polymer dynamics

1 Introduction

Neutron scattering has become an extremely popular experimental tool for probing polymer structure and dynamics [1]. Theoretical methods such as the Random Phase Approximation (RPA) [2,3] have greatly aided the interpretation of scattering results, particularly in systems such as block copolymer melts where both inter- and intrachain correlations need to be modelled correctly. The importance of the RPA is that it provides a crucial link between microscopic models for polymers (*e.g.* the distribution of monomers in a block copolymer) and an expression for the scattering. This paper is concerned with scattering experiments which examine the nature of localising constraints (entanglements and crosslinks) present in polymer melts and networks. These experiments require a derivation of the scattering pattern from microscopic models involving quenched (or very slow) translational degrees of freedom. This paper extends the scope of the RPA to deal with such models.

In polymer networks, the localising constraints are provided by the chemical crosslinks and topological entanglements. The variables associated with these constraints are "quenched" in the truest sense of the word; they are fixed and cannot relax. Any given monomer is constrained to a small region of space about its mean position. It is this physical picture that gave rise to the "tube model" for polymer networks; a polymer chain is confined to a tube-like volume about its mean path [4–7]. Recent experiments [8–10] have aimed to test this "tube model" for polymer networks by straining selectively labelled networks. The application of an external strain is vital to these experiments because the fluctuation volume and mean path are conjectured to have a different coupling to strain.

A second type of experiment is aimed at testing the tube model for strongly stretched polymer melts [11]. The tube model as applied to melts is a dynamical concept which describes the motion of melt chains and how they explore phase space. As in a network, each melt chain is restricted by topological constraints with the surrounding chains. In contrast to the network case, melt chains are not pinned by crosslinks and so are free (eventually) to explore all possible conformations. In this sense, there are no truly "quenched" position variables in polymer melts. However, some of the variables associated with the tube can be extremely slow compared to the experimental timescale, taking many hours to relax. Often it is necessary to treat these variables as though they were effectively quenched.

For example, one recent experiment [12] has aimed to confirm tube model predictions of chain retraction [13–16] and branch-point withdrawal [17] in strongly stretched polymer melts. A melt of H-shaped polymers, such as the one shown in Figure 1, is stretched. It has

[a] e-mail: d.j.read@leeds.ac.uk

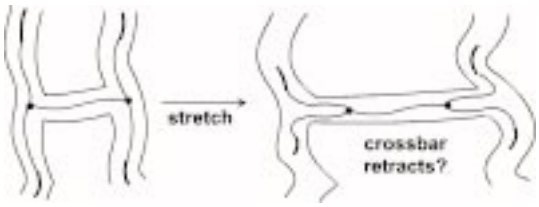

Fig. 1. Illustrating the tube model for a strongly stretched H-polymer. The arms retract to their equilibrium length, but the crossbar retraction may be suppressed because of the branch points. In the polymer shown, the arm ends are deuterated, so crossbar retraction may significantly alter the scattering pattern.

been conjectured that above a certain critical strain, the branch-points withdraw into the central tube section (the driving force for this is provided by the central crossbar, which is stretched above its equilibrium tube contour length). When withdrawal occurs in an H-shaped polymer, the arms (which were originally in separate and independent tube segments) are pulled into the central tube and are thus localised in the same region of space. If the arms in a melt of H-polymers are selectively labelled with deuterium, as shown in Figure 1, then the withdrawal of the branch point significantly increases the correlation between the deuterated segments. It is to be expected that this will have a marked effect on the correlation hole peak in the neutron scattering pattern [18], so that a scattering experiment may be able to confirm the branch-point withdrawal. The experiment requires a stretch, then a rapid temperature quench after one Rouse time to freeze the chains in their retracted positions. Between the stretch and the quench, some of the polymer degrees of freedom have time to relax. The quench suppresses further chain relaxation whilst the scattering takes place.

A simple example to illustrate the effect of quenched variables

Each of the above experiments involve quenched localising constraints on the polymer chains. We now show that a new theory is necessary to deal with these quenched variables, by giving a simple example where a naïve application of the Random Phase Approximation (RPA) gives erroneous results.

Consider an incompressible melt of diblock copolymers comprising monomers of type A and B. We assume, for simplicity, that the Flory interaction parameter between A and B is zero, in which case the collective scattering function for the melt is given by the standard RPA formula;

$$S(\mathbf{q}) = \frac{S^{\mathrm{AA}}_{\mathbf{q}} S^{\mathrm{BB}}_{\mathbf{q}} - \left(S^{\mathrm{AB}}_{\mathbf{q}}\right)^2}{\left(S^{\mathrm{AA}}_{\mathbf{q}} + S^{\mathrm{BB}}_{\mathbf{q}} + 2S^{\mathrm{AB}}_{\mathbf{q}}\right)} \cdot \qquad (1)$$

Let us now suppose, for the sake of example, that it is possible to freeze all the A monomers in their positions, and then change the statistics of the B blocks (*e.g.* "swell" them by a change in Kuhn length). In this example then, the quenched variables are the positions of the A monomers, and the annealed variables are the configurations of the B blocks. A simple application of the RPA to this new system configuration would use equation (1) and obtain structure factors $S^{\mathrm{IJ}}_{\mathbf{q}}$ by treating the annealed average and the quenched average at the same level. It would hence predict a change in the scattering pattern when the B blocks swell, because the structure factors $S^{\mathrm{BB}}_{\mathbf{q}}$ and $S^{\mathrm{AB}}_{\mathbf{q}}$ change. This prediction is that the correlation hole peak moves to smaller $\mathbf{q}$ because the overall size of the diblock has increased.

In fact, the correct result is that the collective scattering is unchanged when the B blocks swell. This is obvious, because the melt is incompressible and the positions of the A monomers are fixed. Whatever the new configurations of the B-monomers, they are forced simply to "fill in the gaps" left by the A-monomers and the overall composition profile is unchanged. The A-monomer positions were determined in the initial melt when the B-blocks were smaller. The naïve application of the RPA through equation (1) fails because it allows the new statistics of the annealed B-blocks to affect the "quenched" statistics of the A-blocks through excluded volume interactions.

The above example involved no stretching of the system. One could equivalently consider what happens if the quenched A monomers are now stretched affinely from their initial positions. By similar reasoning, the new collective scattering pattern is simply the "affinely deformed" scattering pattern of the initial melt before the stretch, *irrespective of the new statistics of the B-block*! It is clear, then, that if quenched variables are involved in a stretched polymer system, then one must take great care when using the RPA to calculate the scattering function.

In fact, it has been known for some time that the standard RPA breaks down when the chains no longer have translational freedom [19,20]. In general, we can say that quenched translational variables tend to preserve something of the scattering pattern from the conditions in which they were quenched. What is required is an "RPA" formula which explicitly distinguishes between the quenched and annealed variables, and which allows the quenched variables to be fixed while the annealed variables fluctuate. This generalised RPA should simplify to the standard RPA results when these quenched variables are absent. This generalisation of the RPA is the central goal of this paper.

We begin by outlining the appropriate physics associated with the localising constraints and their effect on scattering calculations. We then outline the main theoretical results obtained in the generalisation of the RPA (detailed calculations are presented in the Appendices). We shall show that our generalisation of the RPA gives the correct scattering result for the simple example discussed in this section. We present some applications of our result to model systems in which the tube constraints are described by the Warner-Edwards model [7]. Finally, we show in Section 5 that, in calculations of scattering patterns on real systems, there can be a strong disparity between the results of the standard RPA formula and our theory, so that a proper consideration of quenched

variables is vital. We discuss our current understanding of the conditions under which it is important to treat quenched variables correctly.

2 Physical concepts underlying the theory

It is important firstly to stress the physical picture implied by the microscopic models with quenched variables in the experiments described in the Introduction. The following statements can be made and will be used as assumptions in the theoretical development that follows:

1. *Each experiment involves "slow" variables which do not relax on the experimental timescale and "fast" variables which do.* In the case of networks, the distinction between these variables is clear; the slow variables are associated with the fixed crosslinks and the fast variables are the available degrees of freedom of the network chains. In melts, the distinction is less clear, but often in branched polymer melts there is an exponential distribution of tube relaxation times [17,22], so that it is then possible to make a clear division between relaxed and unrelaxed tube variables at a given timescale. In the H-polymer experiment discussed above, the relevant time is that between the stretch and the temperature quench. In our theory, the fast variables are treated as annealed, whilst the slow variables are treated as effectively quenched. Ultimately we average over both quenched and annealed variables (with care as to where the averages are taken). We denote averages over annealed variables by angular brackets, $\langle \dots \rangle$, and averages over quenched variables by an overbar, $\overline{(\dots)}$.
2. *The slow variables were determined in an equilibrium melt situation but are now in a non-equilibrium configuration due to some deformation (e.g. a stretch).* This is one of a set of possible statements which allow us to derive correlations between the quenched "slow" variables. It is an appropriate statement for polymer melts, and networks crosslinked in the melt state. The interactions in the "initial equilibrium melt" (IEM) lead to correlations between the slow variables which are preserved after the deformation. This means that certain aspects of the composition profile before the deformation are "frozen in" after the deformation.
3. *After the deformation, the fast variables fluctuate subject to chain-chain interactions and the constraints imposed by the non-equilibrium slow variables.*

The above considerations force us to deal with the configurations of the "slow" (quenched) and "fast" (annealed) variables separately. We therefore have to use the Random Phase Approximation twice, once to deal with the initial equilibrium melt (IEM) interactions which give correlations between quenched variables, and once to deal with the "post-deformation" (PD) interactions which give correlations between the annealed variables. In the following development, we shall consider only interactions leading to (near) incompressibility. We ignore, for example, the Flory chi parameter between labelled and unlabelled species, assuming the experiment to be designed so that it is negligible.

The strategy for the calculation is as follows. In any single application, the RPA begins with structure factors calculated in the absence of interactions and uses these to calculate the scattering structure factor of the interacting system. The first task then is to use the RPA to find an expression for the scattering function of the interacting melt after the deformation, assuming some prior knowledge of the quenched variables. This input to this application of the RPA will be structure factors calculated in the absence of "post-deformation" (PD) interactions but subject to quenched variables. This RPA application will then include the effect of the PD interactions.

The second task is the calculation of the input structure factors for the first task. In this calculation, "initial equilibrium melt" (IEM) interactions are important in the sense that they affect the distribution of the quenched variables. We define polymer density fields for the chains in the initial equilibrium melt (IEM fields) and other density fields for chains post-deformation (PD fields). These fields are correlated because the quenched variables are preserved during the deformation. We calculate correlation functions between the fields (*i.e.* structure factors) using a microscopic model in the absence of *any* excluded volume interactions. The RPA formalism allows the imposition of interactions onto the IEM density fields, inducing further correlations between the PD fields. In this way, the IEM interactions make their presence felt in the melt after the deformation, through the correlations induced by the quenched variables.

In the following section we outline the main theoretical results which arise from this double application of the RPA formalism. The details of the derivation can be found in the Appendices.

3 Main theoretical results

We shall consider a simple experiment in which an equilibrated isotropic "melt" is deformed, and the tube variables are quenched either by crosslinks or by a temperature quench. The "generalised deformation" may include a stretch described by a tensor $\mathbf{E}$ which transforms an embedded vector $\mathbf{x}$ according to

$$\mathbf{x} \to \mathbf{E} \cdot \mathbf{x}. \tag{2}$$

The discussion in the preceding section indicates that we need to account for both initial equilibrium melt (IEM) and post-deformation (PD) interactions between chains and also define associated polymer density fields.

The PD fields are defined as follows. After the deformation the position of monomer l on chain α is $\mathbf{r}_l^\alpha$, and we define Fourier transformed densities of the labelled (A)

$$S(\mathbf{q}) = \frac{T^{\mathrm{AA}}_{\mathbf{q}} T^{\mathrm{BB}}_{\mathbf{q}} - \left(T^{\mathrm{AB}}_{\mathbf{q}}\right)^2}{\left(T^{\mathrm{AA}}_{\mathbf{q}} + T^{\mathrm{BB}}_{\mathbf{q}} + 2T^{\mathrm{AB}}_{\mathbf{q}}\right)} + \frac{\Delta^{\mathrm{AA}}_{\mathbf{q}} \left(T^{\mathrm{BB}}_{\mathbf{q}} + T^{\mathrm{AB}}_{\mathbf{q}}\right)^2 + \Delta^{\mathrm{BB}}_{\mathbf{q}} \left(T^{\mathrm{AA}}_{\mathbf{q}} + T^{\mathrm{AB}}_{\mathbf{q}}\right)^2 - 2\Delta^{\mathrm{AB}}_{\mathbf{q}} \left(T^{\mathrm{AA}}_{\mathbf{q}} + T^{\mathrm{AB}}_{\mathbf{q}}\right)\left(T^{\mathrm{BB}}_{\mathbf{q}} + T^{\mathrm{AB}}_{\mathbf{q}}\right)}{\left(T^{\mathrm{AA}}_{\mathbf{q}} + T^{\mathrm{BB}}_{\mathbf{q}} + 2T^{\mathrm{AB}}_{\mathbf{q}}\right)^2} \tag{5}$$

monomers and unlabelled (B) monomers as;

$$\rho^{\mathrm{A}}_{\mathbf{q}} = \sum_{\alpha,l} y^{\alpha}_{l} \exp\left(\mathrm{i}\mathbf{q}\cdot\mathbf{r}^{\alpha}_{l}\right) \qquad \rho^{\mathrm{B}}_{\mathbf{q}} = \sum_{\alpha,l} \left(1 - y^{\alpha}_{l}\right) \exp\left(\mathrm{i}\mathbf{q}\cdot\mathbf{r}^{\alpha}_{l}\right) \tag{3}$$

where $y^{\alpha}_{l} = 1$ if the monomer is labelled and $y^{\alpha}_{l} = 0$ otherwise.

Before the deformation, the position of monomer l on chain α is $\mathbf{x}^{\alpha}_{l}$. The most convenient IEM field is the total monomer density of the system after a purely affine transformation of all monomers by the matrix $\mathbf{E}$.

$$\varphi_{\mathbf{q}} = \sum_{\alpha,l} \exp\left(\mathrm{i}\mathbf{q}\cdot\mathbf{E}\cdot\mathbf{x}^{\alpha}_{l}\right). \tag{4}$$

Notice that the sum in $\varphi_{\mathbf{q}}$ is over all A and B monomers. The use of an affine transformation of the $\mathbf{x}^{\alpha}_{l}$ *via* the strain tensor $\mathbf{E}$ in this definition is a convenience which avoids problems with translational symmetry in later averages.

The formal RPA result for the scattering function subject to incompressibility in the melt after the deformation and quenched localising variables is derived in Appendix A. If the Flory interaction parameter, χ, is negligibly small, then the scattering function is of form:

see equation (5) above

where the structure factors $T^{\mathrm{IJ}}_{\mathbf{q}}$ and $\Delta^{\mathrm{IJ}}_{\mathbf{q}}$ will be defined below. This expression represents a generalisation (to account for the existence of correlations between A and B monomers in the structure factors) of a model-dependent result first derived by Brereton and Vilgis [19].

There are two types of structure factor which must be calculated in the above equation (5). The first is of type

$$\Delta^{\mathrm{IJ}}_{\mathbf{q}} = \overline{\left\langle \rho^{\mathrm{I}}_{\mathbf{q}} \right\rangle_0 \left\langle \rho^{\mathrm{J}}_{-\mathbf{q}} \right\rangle_0} \tag{6}$$

where the labels I and J can each be either A or B. The annealed averages $\langle \dots \rangle_0$ are calculated in the absence of PD interactions (denoted by the subscript 0), but subject to quenched localising variables. The average $\overline{(\dots)}$ over these quenched variables must include correlations between the variables due to initial equilibrium melt incompressibility. The structure factors of type $\Delta^{\mathrm{IJ}}_{\mathbf{q}}$ are related to the non-zero mean of the concentration profile due to quenched variables.

The second type of structure factor is:

$$T^{\mathrm{IJ}}_{\mathbf{q}} = \overline{\left\langle \rho^{\mathrm{I}}_{\mathbf{q}} \rho^{\mathrm{J}}_{-\mathbf{q}} \right\rangle_0 - \left\langle \rho^{\mathrm{I}}_{\mathbf{q}} \right\rangle_0 \left\langle \rho^{\mathrm{J}}_{-\mathbf{q}} \right\rangle_0} \tag{7}$$

which is related to fluctuations about the mean of the frozen-in concentration fluctuations, again in the absence of post-stretch interactions.

The two types of structure factor $T^{\mathrm{IJ}}_{\mathbf{q}}$ and $\Delta^{\mathrm{IJ}}_{\mathbf{q}}$ must be calculated subject to correlations between the quenched variables. To do this, we use an RPA calculation which relates $T^{\mathrm{IJ}}_{\mathbf{q}}$ and $\Delta^{\mathrm{IJ}}_{\mathbf{q}}$ to "bare" correlation functions between the density fields $\rho^{\mathrm{A}}_{\mathbf{q}}$, $\rho^{\mathrm{B}}_{\mathbf{q}}$ and $\varphi_{\mathbf{q}}$ in the absence of *any* interactions (in this limit $\varphi_{\mathbf{q}}$ can be non-zero). Note that these fields are correlated because they include the *same* quenched variables. Then, interactions are introduced which enforce incompressibility in the initial equilibrium melt (*i.e.* they enforce $\varphi_{\mathbf{q}} = 0$); these interactions induce further correlations between the density fields $\rho^{\mathrm{A}}_{\mathbf{q}}$ and $\rho^{\mathrm{B}}_{\mathbf{q}}$ which become evident in $T^{\mathrm{IJ}}_{\mathbf{q}}$ and $\Delta^{\mathrm{IJ}}_{\mathbf{q}}$. This calculation is detailed in Appendix B.

There are four important types of "bare" correlation functions;

$$\begin{aligned}
\Delta^{\mathrm{IJ}}_{0\mathbf{q}} &= \overline{\left\langle \rho^{\mathrm{I}}_{\mathbf{q}} \right\rangle_0 \left\langle \rho^{\mathrm{J}}_{-\mathbf{q}} \right\rangle_0}^{0} \\
T^{\mathrm{IJ}}_{0\mathbf{q}} &= \overline{\left\langle \rho^{\mathrm{I}}_{\mathbf{q}} \rho^{\mathrm{J}}_{-\mathbf{q}} \right\rangle_0 - \left\langle \rho^{\mathrm{I}}_{\mathbf{q}} \right\rangle_0 \left\langle \rho^{\mathrm{J}}_{-\mathbf{q}} \right\rangle_0}^{0} \\
D^{\mathrm{I}}_{\mathbf{q}} &= \overline{\left\langle \rho^{\mathrm{I}}_{\mathbf{q}} \right\rangle_0 \left\langle \varphi_{-\mathbf{q}} \right\rangle_0}^{0} \\
S^{\mathrm{tot}}_{\mathbf{q}} &= \overline{\left\langle \varphi_{\mathbf{q}} \varphi_{-\mathbf{q}} \right\rangle_0}^{0}.
\end{aligned} \tag{8}$$

The superscript 0 denotes the absence of correlations induced by excluded volume interactions in the quenched average. The result of the calculation is that

$$\begin{aligned}
T^{\mathrm{IJ}}_{\mathbf{q}} &= T^{\mathrm{IJ}}_{0\mathbf{q}} \\
\Delta^{\mathrm{IJ}}_{\mathbf{q}} &= \Delta^{\mathrm{IJ}}_{0\mathbf{q}} - \frac{D^{\mathrm{I}}_{\mathbf{q}} D^{\mathrm{J}}_{\mathbf{q}}}{S^{\mathrm{tot}}_{\mathbf{q}}}.
\end{aligned} \tag{9}$$

This shows that the IEM incompressibility affects $\Delta^{\mathrm{IJ}}_{\mathbf{q}}$ (which represents composition variations frozen-in by the quenched variables) but not $T^{\mathrm{IJ}}_{\mathbf{q}}$ (which represents composition fluctuations about the frozen-in mean). This is because $\Delta^{\mathrm{IJ}}_{\mathbf{q}}$ includes chain-chain correlations, whilst $T^{\mathrm{IJ}}_{\mathbf{q}}$ includes only same-chain terms.

Together, the equations (5, 8, 9) represent the generalisation of the standard RPA result to the deformed melt with quenched but correlated variables. As in the standard RPA case, the structure factors in (8) must be calculated from some convenient and appropriate model for the polymer melt.

It is worth noting that for an equilibrated melt (where there are no quenched variables), translational symmetry applies and $\left\langle \rho^{\mathrm{I}}_{\mathbf{q}} \right\rangle_0 = 0$. In this case the structure factors reduce to $\Delta^{\mathrm{IJ}}_{\mathbf{q}} = 0$ and $T^{\mathrm{IJ}}_{\mathbf{q}} = S^{\mathrm{IJ}}_{\mathbf{q}} = \left\langle \rho^{\mathrm{I}}_{\mathbf{q}} \rho^{\mathrm{J}}_{-\mathbf{q}} \right\rangle_0$.

Equation (5) is then identical to the standard RPA result for the melt scattering function of equation (1).

Furthermore, if the melt is not deformed, then the $\{\mathbf{x}_l^\alpha\}$ and the $\{\mathbf{r}_l^\alpha\}$ are equivalent (in that they both fluctuate within identical equilibrium quenched variables). We can then make the substitution $\varphi_{\mathbf{q}} \to \rho_{\mathbf{q}}^{\mathrm{A}} + \rho_{\mathbf{q}}^{\mathrm{B}}$ in the bare correlation functions, so that

$$\begin{aligned} D_{\mathbf{q}}^{\mathrm{A}} &\to \Delta_{0\mathbf{q}}^{\mathrm{AA}} + \Delta_{0\mathbf{q}}^{\mathrm{AB}} \\ D_{\mathbf{q}}^{\mathrm{B}} &\to \Delta_{0\mathbf{q}}^{\mathrm{BB}} + \Delta_{0\mathbf{q}}^{\mathrm{AB}} \\ S_{\mathbf{q}}^{\mathrm{tot}} &\to S_{0\mathbf{q}}^{\mathrm{AA}} + S_{0\mathbf{q}}^{\mathrm{BB}} + 2S_{0\mathbf{q}}^{\mathrm{AB}} \end{aligned} \tag{10}$$

where

$$S_{0\mathbf{q}}^{\mathrm{IJ}} = T_{0\mathbf{q}}^{\mathrm{IJ}} + \Delta_{0\mathbf{q}}^{\mathrm{IJ}} = \overline{\left\langle \rho_{\mathbf{q}}^{\mathrm{I}} \rho_{-\mathbf{q}}^{\mathrm{J}} \right\rangle_0}^0 . \tag{11}$$

Substituting these into (5, 9) also yields the incompressible melt scattering function given above in equation (1). This is to be expected because the quenched variables are in an equilibrium configuration. In the general case where stretching and retraction occurs we cannot make this simplification and we must retain the formal separation between the quenched and annealed variables. A third important limit of the equations (5, 8, 9), in the situation where A and B chains are statistically identical, is dealt with in Appendix C.

The simple example revisited

We now return to the simple example given in the introduction in which the A-monomers on a diblock are completely quenched and the B-monomers are allowed to "swell". We shall show that our expression for the scattering (5, 8, 9) gives the correct result, that the scattering is unchanged by the B-block swelling.

The variables associated with the A-blocks are entirely quenched, so there are no annealed A-variables and $T_{\mathbf{q}}^{\mathrm{AA}} = T_{\mathbf{q}}^{\mathrm{AB}} = 0$. This greatly simplifies our scattering expression and we find

$$S(\mathbf{q}) = \Delta_{\mathbf{q}}^{\mathrm{AA}} = \Delta_{0\mathbf{q}}^{\mathrm{AA}} - \frac{\left(D_{\mathbf{q}}^{\mathrm{A}}\right)^2}{S_{\mathbf{q}}^{\mathrm{tot}}} . \tag{12}$$

Because the A monomers are quenched in their initial equilibrium melt (IEM) positions, the structure factors in the above expression simplify to IEM structure factors

$$\begin{aligned} \Delta_{0\mathbf{q}}^{\mathrm{AA}} &= S_{\mathrm{IEM}}^{\mathrm{AA}} \\ D_{\mathbf{q}}^{\mathrm{A}} &= S_{\mathrm{IEM}}^{\mathrm{AA}} + S_{\mathrm{IEM}}^{\mathrm{AB}} \\ S_{\mathbf{q}}^{\mathrm{tot}} &= S_{\mathrm{IEM}}^{\mathrm{AA}} + S_{\mathrm{IEM}}^{\mathrm{BB}} + 2S_{\mathrm{IEM}}^{\mathrm{AB}} \end{aligned} \tag{13}$$

and we correctly predict the scattering to be identical to the initial melt.

$$S(\mathbf{q}) = \frac{S_{\mathrm{IEM}}^{\mathrm{AA}} S_{\mathrm{IEM}}^{\mathrm{BB}} - \left(S_{\mathrm{IEM}}^{\mathrm{AB}}\right)^2}{\left(S_{\mathrm{IEM}}^{\mathrm{AA}} + S_{\mathrm{IEM}}^{\mathrm{BB}} + 2S_{\mathrm{IEM}}^{\mathrm{AB}}\right)} . \tag{14}$$

This simple example is extreme in the sense that the localisation of the A monomers is absolute – they are fixed in their initial positions. Nevertheless, it illustrates the dangers of failing to consider the implications of quenched variables at all stages of a scattering calculation. In more realistic situations our expression allows for fluctuation of monomers about their mean positions through the structure factors $T_{\mathbf{q}}^{\mathrm{IJ}}$ whilst retaining some of the freezing in of the composition profile due to quenched variables through the $\Delta_{\mathbf{q}}^{\mathrm{IJ}}$.

4 Example applications

4.1 Structure factors from the Warner-Edwards tube model

We now demonstrate the application of the above RPA theory for the calculation of the scattering functions for some block copolymer systems. In these systems, the Warner-Edwards picture of the tube [7] is used to model the quenched localising constraints in melts and networks.

The Warner-Edwards (W-E) model was originally proposed as simplified model for chains in polymer networks. The localising effect of crosslinks and physical entanglements was modelled by placing each monomer l in its own harmonic potential (centred on $\mathbf{R}(l)$), giving a free energy functional for the chain (in units of $k_{\mathrm{B}}T$) as:

$$F_{\mathbf{R}}\{\mathbf{r}(l)\} = \frac{1}{2}\sum_l \left\{ \frac{3}{b^2}\left(\frac{\partial \mathbf{r}(l)}{\partial l}\right)^2 + \frac{2b^2}{d^4}\left[\mathbf{r}(l) - \mathbf{R}(l)\right]^2 \right\} \tag{15}$$

where the position of monomer l is $\mathbf{r}(l)$ and d is the typical deviation of a monomer from its mean position. The $\mathbf{R}(l)$ define a "tube" in the sense that they define a mean path for the network chain. A stretch may be imposed by affine transformation of the $\mathbf{R}(l)$.

We have shown recently [23] that the W-E model may be solved exactly by considering the normal modes of the chain under the harmonic potentials:

$$\begin{aligned} \mathbf{r}(l) &= \sum_p \mathbf{r}_p \exp(\mathrm{i}lp) \\ \mathbf{R}(l) &= \sum_p \mathbf{R}_p \exp(\mathrm{i}lp) . \end{aligned} \tag{16}$$

These variables diagonalise the free energy functional, and allow the explicit calculation of scattering functions for network chains.

Since the W-E model is simple and can be solved exactly, it is attractive to apply the model to calculate scattering functions for entangled polymer melts (*e.g.* for the H-polymer experiment described in the introduction). However, for melt experiments the W-E description of the tube is less obviously applicable. This is because mechanisms such as reptation or chain retraction allow the movement of the chain along its tube, a motion that is

impossible if each monomer sits in a local harmonic potential. Experimental timescales may be designed to suppress much of this motion (especially if the molecules are branched), but chain retraction is thought to be fast (*i.e.* within one chain Rouse time) even in branched polymers. If the W-E model is to be applied to melts, then it is necessary at the very least to include the phenomenon of chain retraction in the model.

Chain retraction was first predicted for linear melt chains by Doi and Edwards [13–16]. They made two assumptions about the way the tube deforms under macroscopic step strain; (i) that the tube path deforms affinely and (ii) that the tube diameter remains constant. Futhermore, they supposed (for the purposes of tractability) that the chain is sufficiently long that its tube mean path samples many different orientations. Then, under a strain tensor $\mathbf{E}$, the length of the tube increased by a factor $\alpha(\mathbf{E}) = \langle|\mathbf{E}\cdot\mathbf{u}|\rangle$ where the average is over all possible direction vectors, $\mathbf{u}$, of the local tube mean path. If the tube diameter remains constant, then the equilibrium tube length of the chain also remains constant. So, whilst the chain initially deforms with its surrounding tube, this deformation gives it a contour length which is larger than its equilibrium value. Doi and Edwards predicted that a linear chain should retract back within the tube by the factor $\alpha(\mathbf{E})$ to reach its equilibrium length.

With the assumption that chain retraction occurs along the tube mean path, we now seek the closest possible analogue to the mean path in the W-E model. For a given set of harmonic potentials $\mathbf{R}(l)$, the chain mean path is given by the chain position, $\mathbf{r}(l) = \hat{\mathbf{r}}(l)$, which minimises the free energy functional of equation (15). In terms of the chain normal modes, p, this minimum energy position is;

$$\hat{\mathbf{r}}_p = \frac{\mathbf{R}_p}{\left(1+\frac{3p^2d^4}{2b^4}\right)}\cdot \tag{17}$$

We now consider how the mean path changes for a chain trapped in a tube which undergoes a stretch given by the matrix $\mathbf{E}$. The tube length increases by the factor $\alpha(\mathbf{E})$, but if chain retraction occurs, the length of the chain mean path might increase only by a factor β. The ratio of these two terms is the degree of retraction, γ.

$$\gamma = \frac{\alpha(\mathbf{E})}{\beta}\cdot \tag{18}$$

A uniform retraction along the tube mean path (which has deformed affinely) may be imposed in the Warner-Edwards model by prescribing a transformation of the chain mean path $\hat{\mathbf{r}}(l)$ *via*

$$\hat{\mathbf{r}}(l) \to \mathbf{E}\cdot\hat{\mathbf{r}}\left(\frac{l}{\gamma}\right). \tag{19}$$

The retraction is represented by "sliding" the monomer l to the initial position in the tube of the (l/γ)th monomer. This level of treatment is similar to that used by Boué, Osaki and Ball in calculating the full structure factor of a retracted chain [21]. The Warner-Edwards formalism, however, gives a slightly different crossover between wavevectors above and below the inverse tube diameter, and allows us to calculate all the required structure factors for our theory.

In terms of the normal modes;

$$\hat{\mathbf{r}}_p \to \mathbf{E}\cdot\hat{\mathbf{r}}_{\gamma p}. \tag{20}$$

This prescription enables the calculation of all the correlation functions of form $T^{\mathrm{IJ}}_{0\mathbf{q}}$, $\Delta^{\mathrm{IJ}}_{0\mathbf{q}}$ and $D^{\mathrm{I}}_{\mathbf{q}}$ for a polymer in a W-E tube.

For a chain of overall molecular weight N we use a normalised wavevector $Q_\mu = q_\mu b\sqrt{N/6}$. We also introduce the normalised tube diameter $\zeta^2 = \frac{\sqrt{6}d^2}{2Nb^2}$ and the contour length co-ordinates $x = l/N$, $y = l'/N$. If the degree of retraction is γ then the bare correlation functions are of form

$$T_{0\mathbf{q}} = nN^2\int \mathrm{d}x\int \mathrm{d}y\,\Theta_1(x,y) \tag{21}$$

$$\Delta_{0\mathbf{q}} = nN^2\int \mathrm{d}x\int \mathrm{d}y\,\Theta_2(x,y) \tag{22}$$

$$D_{\mathbf{q}} = nN^2\int \mathrm{d}x\int \mathrm{d}y\,\Theta_3(x,y) \tag{23}$$

where

$$\Theta_1(x,y) = \exp\left[-\sum_\mu Q_\mu^2\lambda_\mu^2\left\{\frac{|x-y|}{\gamma}-\zeta^2\left(1-\exp\left(-\frac{|x-y|}{\gamma\zeta^2}\right)\right)\right\}\right] \times\left\{\exp\left[-\sum_\mu Q_\mu^2\zeta^2\left(1-\exp\left(-\frac{|x-y|}{\zeta^2}\right)\right)\right] -\exp\left[-\sum_\mu Q_\mu^2\zeta^2\right]\right\} \tag{24}$$

$$\Theta_2(x,y) = \exp\left[-\sum_\mu Q_\mu^2\zeta^2 + Q_\mu^2\lambda_\mu^2\left\{\frac{|x-y|}{\gamma} -\zeta^2\left(1-\exp\left(-\frac{|x-y|}{\gamma\zeta^2}\right)\right)\right\}\right] \tag{25}$$

$$\Theta_3(x,y) = \exp\left[-\sum_\mu Q_\mu^2\zeta^2\left(\frac{1+\lambda_\mu^2}{2}\right) + Q_\mu^2\lambda_\mu^2\left\{\left|\frac{x}{\gamma}-y\right| -\zeta^2\left(1-\exp\left(-\frac{1}{\zeta^2}\left|\frac{x}{\gamma}-y\right|\right)\right)\right\}\right]. \tag{26}$$

In all of these expressions, the range of integration for the contour length co-ordinates must be chosen to reflect the required correlation function. For example, in calculating $T^{\mathrm{AB}}_{0\mathbf{q}}$ the x integral should be over all A monomers and the y integral over all B monomers. We have included the prefactor nN^2 which converts from the single chain structure

factors to the many-chain bare correlation functions (n is the number of chains, N is their degree of polymerisation).

Each of the above expressions has a term in the exponential of form

$$\sum_\mu Q_\mu^2 \lambda_\mu^2 \left\{ \frac{|x-y|}{\gamma} - \zeta^2 \left(1 - \exp\left(-\frac{|x-y|}{\gamma\zeta^2} \right) \right) \right\}.$$

This is related to correlations along the deformed mean path of the chain, which is affected both by the affine deformation (through λ_μ^2) and the retraction (through γ). In $D_{\mathbf{q}}$, the form is subtly different, $\frac{|x-y|}{\gamma}$ being replaced by $\left| \frac{x}{\gamma} - y \right|$. This is because $D_{\mathbf{q}}$ represents correlations between the chain before and after stretching. The chain before the stretch occupied the whole length of the tube and was not retracted, so that $\gamma = 1$. The chain after the stretch is retracted. In the expression for $D_{\mathbf{q}}$, the x contour variable relates to the chain after the stretch, and the y contour variable relates to the chain before the stretch. Care must be taken to ensure that the point $x = y = 0$ is taken to be at a monomer which does not change position within the tube under the retraction (in a symmetric polymer this point is at the centre).

The remainder of the three expressions relate to fluctuations of the chain within the tube. Unless the tube diameter couples to the stretch, these fluctuations are isotropic and unaffected by the deformation, the only apparent exception being the factor $\left(1 + \lambda_\mu^2\right)/2$ in $D_{\mathbf{q}}$. This factor arises mathematically because the unstretched chain fluctuates isotropically in its tube, but the order parameter $\varphi_{\mathbf{q}}$ incorporates an affine deformation of the unstretched state, to bring the $\mathbf{x}_l^\alpha$ into the same space as the $\mathbf{r}_l^\alpha$. This deformation applies both to the fluctuations within the tube and to the tube mean path, giving the extra factor $\lambda_\mu^2/2$. Physically this arises because when we consider the correlations between the stretched and unstretched chain, the stretch amplifies any initial deviations of the chain from its mean path.

The final correlation function to be calculated in (8) is $S_{\mathbf{q}}^{\mathrm{tot}} = \overline{\langle \varphi_{\mathbf{q}} \varphi_{-\mathbf{q}} \rangle_{0,\mathbf{x}}}^{0}$. If all the chains are identical, this is simply proportional to the standard single chain structure factor $g(\mathbf{q})$, (the Debye function if the chains are linear), but affinely deformed *via* $\mathbf{E}$;

$$S_{\mathbf{q}}^{\mathrm{tot}} = nN^2 g(\mathbf{q} \cdot \mathbf{E}). \tag{27}$$

Note that this structure factor includes all A and B monomers.

4.2 Scattering from stretched triblock copolymers

As an example of the application of the Warner-Edwards model to our modified RPA theory, we calculate the scattering function of a stretched melt of symmetric triblock copolymers, entirely confined to a Warner-Edwards tube. The central portion, a fraction f of the polymer, is labelled. This yields the following expressions for the structure factors $T_{0\mathbf{q}}^{\mathrm{IJ}}$, $\Delta_{0\mathbf{q}}^{\mathrm{IJ}}$ and $D_{\mathbf{q}}^{\mathrm{I}}$:

$$T_{0\mathbf{q}}^{\mathrm{AA}} = 2nN^2 \left[\int_{\frac{f}{2}}^{\frac{1}{2}} \mathrm{d}x \int_{\frac{f}{2}}^{\frac{1}{2}} \mathrm{d}y\, \Theta_1(x,y) + \int_{-\frac{1}{2}}^{-\frac{f}{2}} \mathrm{d}x \int_{\frac{f}{2}}^{\frac{1}{2}} \mathrm{d}y\, \Theta_1(x,y) \right] \tag{28}$$

$$\Delta_{0\mathbf{q}}^{\mathrm{AA}} = 2nN^2 \left[\int_{\frac{f}{2}}^{\frac{1}{2}} \mathrm{d}x \int_{\frac{f}{2}}^{\frac{1}{2}} \mathrm{d}y\, \Theta_2(x,y) + \int_{-\frac{1}{2}}^{-\frac{f}{2}} \mathrm{d}x \int_{\frac{f}{2}}^{\frac{1}{2}} \mathrm{d}y\, \Theta_2(x,y) \right] \tag{29}$$

$$T_{0\mathbf{q}}^{\mathrm{BB}} = nN^2 \int_{-\frac{f}{2}}^{\frac{f}{2}} \mathrm{d}x \int_{-\frac{f}{2}}^{\frac{f}{2}} \mathrm{d}y\, \Theta_1(x,y) \tag{30}$$

$$\Delta_{0\mathbf{q}}^{\mathrm{BB}} = nN^2 \int_{-\frac{f}{2}}^{\frac{f}{2}} \mathrm{d}x \int_{-\frac{f}{2}}^{\frac{f}{2}} \mathrm{d}y\, \Theta_2(x,y) \tag{31}$$

$$T_{0\mathbf{q}}^{\mathrm{AB}} = 2nN^2 \int_{-\frac{f}{2}}^{\frac{f}{2}} \mathrm{d}x \int_{\frac{f}{2}}^{\frac{1}{2}} \mathrm{d}y\, \Theta_1(x,y) \tag{32}$$

$$\Delta_{0\mathbf{q}}^{\mathrm{AB}} = 2nN^2 \int_{-\frac{f}{2}}^{\frac{f}{2}} \mathrm{d}x \int_{\frac{f}{2}}^{\frac{1}{2}} \mathrm{d}y\, \Theta_2(x,y) \tag{33}$$

$$D_{\mathbf{q}}^{\mathrm{A}} = 2nN^2 \int_{\frac{f}{2}}^{\frac{1}{2}} \mathrm{d}x \int_{-\frac{1}{2}}^{\frac{1}{2}} \mathrm{d}y\, \Theta_3(x,y) \tag{34}$$

$$D_{\mathbf{q}}^{\mathrm{B}} = nN^2 \int_{-\frac{f}{2}}^{\frac{f}{2}} \mathrm{d}x \int_{-\frac{1}{2}}^{\frac{1}{2}} \mathrm{d}y\, \Theta_3(x,y). \tag{35}$$

These are substituted into equations (5, 9) to give the total scattering function.

Figure 2 shows plots of the predicted structure factor for a uniaxial stretch of $\lambda_z = 3$, $\lambda_x = \lambda_y = 1/\sqrt{3}$. The scattering function for an isotropic melt is shown for comparison. The curves marked with an "a" are for a tube diameter much smaller than the chain ($\zeta^2 = 0.01$, which corresponds to about 100 "entanglements" per chain) in the "network" limit of $\gamma = 1$ (*i.e.* no retraction). In this limit, the deformation is almost affine, and the parallel and perpendicular peaks are nearly affine transformations of the unstretched scattering function. If the tube diameter is larger, as in the curves marked with a "b" ($\zeta^2 = 0.09$, which corresponds to about 11 "entanglements" per chain), then there is a strong effect on the scattering function. At higher $Q \gtrsim 1/\zeta$, the scattering both parallel and perpendicular to the stretch is closer to the unstretched melt value, indicating that on lengthscales smaller than the tube diameter the "network" becomes more isotropic. This significantly reduces the correlation hole peak perpendicular to the stretch, and moves it to smaller wavevectors. At lower Q, the scattering is less affected by the change in tube diameter; the correlation hole peak parallel to the stretch stays in almost the same place and increases a little in magnitude. The curves marked with a "c" in Figure 2 are triblock scattering functions in the limit of full chain

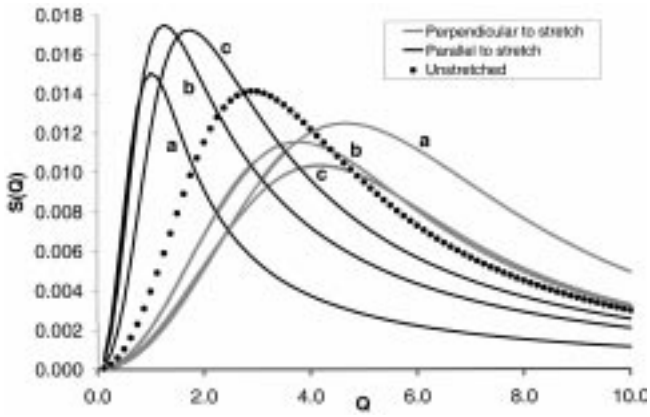

Fig. 2. Predicted parallel and perpendicular scattering for a stretched melt of triblock copolymers confined to a Warner-Edwards tube. Parameters (see text) are $\lambda_z = 3$, $\lambda_x = \lambda_y = 1/\sqrt{3}$, $f = 0.2$, and for curves "a" $\gamma = 1$ (*i.e.* no retraction), $\zeta^2 = 0.01$, for curves "b" $\gamma = 1$ (*i.e* no retraction), $\zeta^2 = 0.09$ and for curves "c" $\gamma = \alpha(\mathbf{E})$ (*i.e.* full retraction), $\zeta^2 = 0.09$.

retraction, $\gamma = \alpha(\mathbf{E})$. The scattering at high $Q \gtrsim 1/\zeta$ is even more isotropic than for the unretracted polymer; the chain retraction allows increased orientational relaxation of the melt on lengthscales smaller than the tube diameter. The correlation hole peak parallel to the stretch moves to higher Q, as would be expected since chain retraction decreases the overall chain dimensions.

These curves illustrate well the separation of lengthscales brought about by the imposition of the tube localising constraints. On large lengthscales, the correlation hole peak is determined almost entirely by tube-tube correlations that were present in the melt or network prior to the stretch. On lengthscales smaller than the tube (*i.e.* the size of the localising constraint) the melt is free to reorient, and the composition profile fluctuates subject to incompressibility.

The above calculation represents the simplest possible tube model for a stretched melt of triblock copolymers. It has recently been demonstrated [24] that within the timescale associated with chain retraction a significant portion of a linear chain escapes from the tube by the process of contour length fluctuation. It is to be expected that this will significantly alter the scattering, and it should be included along with chain retraction in a scattering calculation. So, whilst the above model is good for illustrative purposes, it is unlikely to provide a good fit to experimental data (for which more detail would be necessary, with the associated increase in volume of algebra).

The model may be better at describing scattering from a crosslinked blend of triblock copolymers, though the only such experiment to date [9] involved detectable chain scission in the scattering. A proper treatment of chain scission needs to distinguish between chains which are scissioned before and chains which are scissioned after being crosslinked to the network. The former are free to explore a "diffusion volume" before being attached to the network, whilst the latter only contribute "dangling ends" to the calculation [25]. Such a treatment of chain scission requires considerable algebra and is beyond the scope of this paper. It should be noted that the theory used by Westermann *et al.* [9] to fit their data did not treat scission in this way. Furthermore, it involved an illegitimate modification to the Warner-Edwards scattering result [23]. Finally, their modification of the RPA is assymmetric under interchange of labelled and unlabelled monomers, which is incorrect for an incompressible system. It is thus doubtful whether there is any reasonable link between their proposed microscopic model and their scattering formula.

4.3 Scattering from an H-shaped-copolymer melt

The theory developed in this paper was originally intended to model the scattering experiment on H-shaped polymers [12] outlined in the introduction and illustrated in Figure 1. The experiment was designed to test the tube model for branched polymer melts, particularly the prediction of branch point withdrawal at large strains. The original prediction of branchpoint withdrawal [17] suggested that it should not occur unless

$$\alpha(\mathbf{E}) \geq 2 \tag{36}$$

at which point the tension in the "crossbar" of the polymer is sufficient to pull the arms into the central tube. This requires uniaxial stretches of $\lambda \gtrsim 4$. Above this strain, it was suggested by McLeish [18] that the altered configuration of the H-polymer (in particular, the localisation of deuterated polymer in the same tube segment) should lead to an increase in the scattering peak.

The tube model assumes (i) that the tube deforms affinely under a strain, (ii) that the tube diameter does not couple to the stretch and (iii) that all polymers retract by the same degree. The last assumption is made partly for the convenience of being able to preaverage the chain retraction, and is justified by saying that all chains sample a large number of different local tube orientations. It was important to take these assumptions and use them to calculate, as accurately as possible, the scattering pattern. This was so that any comparison of the predicted and experimental scattering might be viewed as a proper test of the assumptions of the microscopic model *i.e.* of the tube model. These assumptions are implicit in the above calculations (particularly in the derivation of structure factors from the Warner-Edwards tube model).

Details of the experiment have been published elsewhere [12]. Briefly, a melt of 1,4 polyisoprene (96%-cis) H-polymers was solution-cast to a thickness of approximately half a millimetre. Solvent was extracted by leaving the samples under vacuum for a week. A rectangle 3 cm $\times$ 1 cm was cut from the sample and clamped at both ends so that the section of polymer to be stretched was 1cm$\times$1cm. The polymer was stretched rapidly by manually pulling the grips apart (the degree of extension being controlled by an "end-stop" with a triggered holding catch). Immediately after the stretch, the sample was plunged into liquid nitrogen to achieve the temperature quench, before being

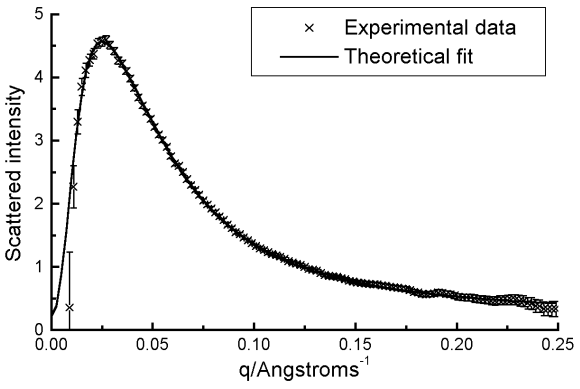

Fig. 3. Experimental neutron scattering from an unstretched melt of 1,4 polyisoprene (96%-cis) H-polymers with parameters $f_{\rm A} = 0.125$ and $f_{\rm cross} = 0.346$ and total molecular weight 3.21×10^5. Also shown is a theoretical fit to the data based on standard RPA theory [27].

transferred to a helium cryostat for the scattering. It is estimated that the total time for stretching plus temperature quench was of the order of 0.1 s. From this description, it is apparent that the extension time is subject to a certain degree of error, but it can be argued that, since the relaxation time of arm segments is exponential in the tube contour length from the free end [22], only order-of-magnitude control in the stretching time is necessary to achieve a small error in the fraction the polymer that has relaxed. Nevertheless, greater control in the experiment is desirable, and this experiment should be viewed as preliminary work for more detailed and careful experiments. In fact, under the experimental conditions (mainly due to the parallel scattering peak impinging on the beam-stop), it was possible only to obtain one useful set of data at a strain ($\lambda_z = 2.3$) which is theoretically too small to give branchpoint withdrawal.

The relevant parameterisation of the polymer is as follows. The end of each arm of the H-polymer is deuterated, so it contains a total fraction $f_{\rm A}$ of deuterated "A" monomers and $(1 - f_{\rm A})$ undeuterated "B" monomers. The interactions of the two monomer types are almost identical and the total deuterium fraction is small, so that the Flory interaction parameter χ is negligible. The "crossbar" is a fraction $f_{\rm cross}$ of the total polymer. For the polymer used in the experiment, $f_{\rm A} = 0.125$ and $f_{\rm cross} = 0.346$ and the total molecular weight 3.21×10^5.

For an unstretched melt of H-polymers, the above theory of Section 3 reduces to the standard RPA. The theoretical scattering from an unstretched melt of H-polymers was derived in an earlier paper [27]. Figure 3 shows a fit to experimental data [12]. We write the normalised wavevector as $Q = qb\sqrt{N/6} = qR_{\rm g}$ where $R_{\rm g}$ is the radius of gyration for a linear polymer of identical molecular weight to the H-polymer. The fit to data is excellent, and gives a value for $R_{\rm g} = 169$ Å which was used as a fixed parameter in all subsequent fits.

When deriving the scattering functions for the stretched H-polymer it was desirable to account for as much as is known about the configurations of stretched branched polymers from rheological studies. One complication is that on the timescale of the experiment, a certain fraction of the arm length (a fraction $f_{\rm dangle}$ of the total molecule for each arm) relaxes and becomes isotropic through the action of star-like breathing modes [22]. On this timescale, these "dangling ends" are effectively free of the tube constraints. The dangling ends were treated as being isotropic at the same level as those in our papers on network dangling ends [23,26]. Corrections were also made to the theory to allow for the expected tube dilation due to constraint release [22] which occurs because the dangling ends move too rapidly to provide effective entanglements with the remaining polymer. Furthermore, whilst early theories for retraction in H-shaped polymers [17] predict no branch point withdrawal at low strains for which $\alpha(\mathbf{E}) < 2$, some withdrawal due to local cage effects is theoretically possible. Therefore, the degree of retraction of the crossbar was considered a variable parameter.

The discussion of scattering functions for retracted polymers, calculated from the Warner-Edwards model in Section 4.1 above, did not cover some of the features seen in the retraction of a branched polymer. The equations given cover only the case of a single chain in a tube retracted by a degree, γ. In the branched polymer case we have further complications; (i) correlations must be calculated for a chain in the same tube but retracted by different degrees at either side of a branch point (in general $\gamma_{\rm cross} \neq \gamma_{\rm arm}$) and (ii) after branch point withdrawal there are sections of tube containing two chain sections, joined at a single end (see Fig. 1). Direct calculation from the Warner-Edwards model of scattering functions is not straightforward in this situation. We can, however, make sensible modifications to the results of (21, 22, 23) based on the separation of these formulae into contributions from the tube mean path (which is well defined) and fluctuations within the tube, which we take to be isotropic. The full derivation of expressions for the correlation functions is then extremely lengthy but manageable. All that is required is counting of all the relevant monomers in each correlation function. We shall not present the full expressions here, as they are extremely unwieldy, but as an example we outline the calculation of $T_{0\mathbf{q}}^{\rm AB}$ in Appendix D.

In Figures 4 and 5 we show theoretical predictions for the scattering at uniaxial stretches of $\lambda_z = 2$, 3, 4 and 5, using the prescription for arm retraction and branchpoint withdrawal given in reference [17] (*i.e.* arm retraction but no branch-point withdrawal for $\lambda < 4$, branchpoint withdrawal for $\lambda \gtrsim 4$). The series of pictures indicate that, qualitatively, the scattering parallel to the stretch increases with increasing strain, with a peak that moves to smaller wavevector. Perpendicular to the stretch, the scattering peak is weakly affected by the strain, until $\lambda \gtrsim 4$ when the peak height begins to increase more rapidly with strain. In all cases, at large wavevectors (*i.e.* probing lengthscales of the order of the tube diameter or smaller) the scattering is much more isotropic than at low

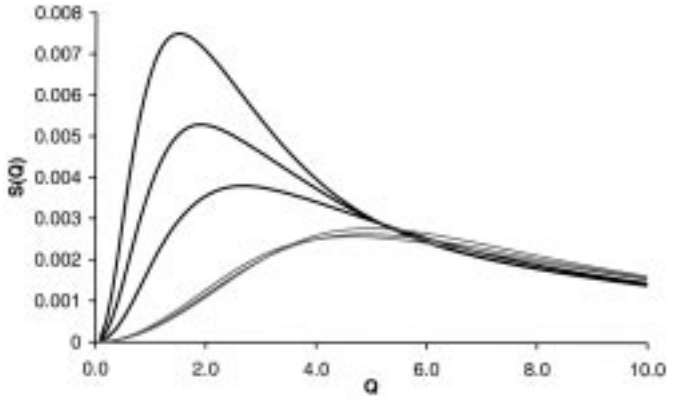

Fig. 4. Predicted scattering parallel (thick black lines) and perpendicular (thin grey lines) to stretches of $\lambda_z = 2, 3$ and 4 from a melt of H-polymers with parameters $f_A = 0.125$, $f_{cross} = 0.346$, $f_{dang} = 0.346$ and $\zeta^2 = 0.0153$. The height of the scattering peak increases with increasing λ_z both parallel and perpendicular to the stretch.

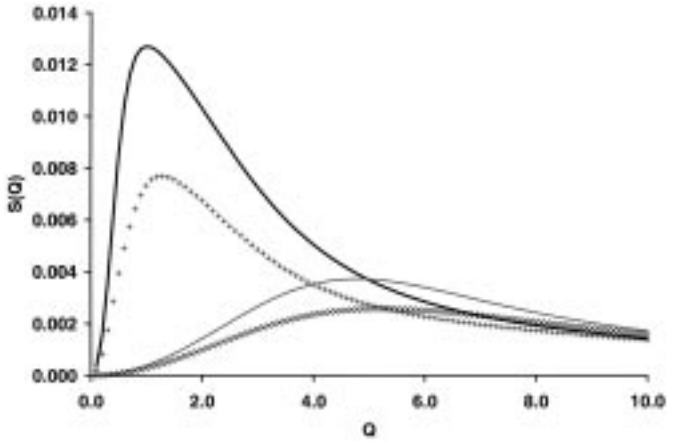

Fig. 5. Predicted scattering parallel (thick black line) and perpendicular (thin grey line) to a stretch of $\lambda_z = 5$ from a melt of H-polymers with parameters $f_A = 0.125$, $f_{cross} = 0.346$, $f_{dang} = 0.346$ and $\zeta^2 = 0.0153$. Also shown is the scattering parallel (+) and perpendicular (×) in the absence of branch-point withdrawal.

wavevectors, indicating near isotropy of chains at small lengthscales.

The most important effect to assess is the effect of branch-point withdrawal on the scattering. Figure 5 ($\lambda_z = 5$) shows a comparison of the predicted scattering for the cases with and without branch-point withdrawal. It is evident that, so long as a large enough range of wavevectors are probed, it should be possible in theory to detect the withdrawal simply from the shape of the curves. At large wavevectors the scattering is independent of the branch-point withdrawal, whereas at lower wavevectors the scattering peaks are much higher for withdrawn branch-points. This is in accord with the basic ideas suggested by McLeish [18]. In the absence of a large spread of wavevectors, one must either be certain to normalise the scattering intensities correctly (so that the withdrawal

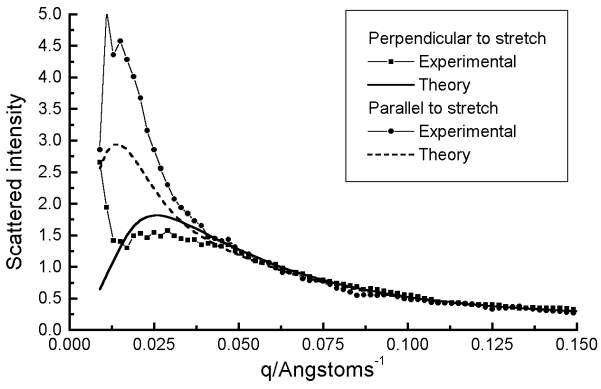

Fig. 6. Experimental neutron scattering from a stretched melt ($\lambda_z = 2.3$) of 1,4 polyisoprene (96%-cis) H-polymers with parameters $f_A = 0.125$ and $f_{cross} = 0.346$ and total molecular weight 3.21×10^5. Also shown is a theoretical fit to the data based on the generalised RPA theory together with a Warner-Edwards tube model (see text for details).

is evident from the increase in absolute scattering peak intensities) or one must look for other distinguishing features of the curves. For example, branch-point withdrawal gives a difference in peak wavevector parallel to the stretch of the order of 20%. The ratio of peak height perpendicular and parallel to the stretch is also a function of the branch-point withdrawal (with our chosen parameters the ratio is 3.4 for withdrawal, but only 3.0 for no withdrawal). All of this should serve to illustrate that the scattering curves are sensitive to the molecular configurations of the H-polymer, so that scattering is indeed a viable probe.

Comments on the fit to experimental results

In Figure 6 is a graph of the experimental neutron scattering [12] from a melt of H-polymers at a uniaxial stretch of $\lambda_z = 2.3$. The scattering is shown both parallel and perpendicular to the stretch. Even though this does not theoretically probe high enough strains to test branch-point withdrawal, it is worth checking to see how well the current microscopic model predicts the scattering. We show a theoretical fit to the curves, using the most likely values for the tube diameter and dangling end fraction obtained from fits to rheological data ($f_{dangle} = 0.08$, $\zeta^2 = 0.0153$).

The derivation of the theoretical curves is based on the assumptions of the tube model outlined above for stretched melts of branched polymers. The arms were assumed to have retracted to their equilibrium tube length. Whilst the tube model at its simplest level [17] does not predict any branchpoint withdrawal at $\lambda_z = 2.3$, allowance is made for partial withdrawal of the branch point into the central crossbar tube, by a distance of the order of the tube diameter, due to local cage effects.

It can be seen that whilst the theory reproduces some of the features of the experimental scattering, the overall quality of the fit is poor. At high scattering wavevectors, the scattering is almost isotropic, which is a result

of the combined effect of isotropic fluctuations within the tube and the dangling ends. This feature is reproduced well by the theory. However, the correlation hole peaks, and notably the large difference between the perpendicular and parallel scattering is not well modelled.

We have attempted to constrain the many parameters in the model to likely values from rheology, but it is possible to allow for some variation in these parameters. Within the model we are able to vary the tube diameter, the dangling-end fraction, the arm retraction or the degree of branch point withdrawal. Whilst it is possible to fit either the perpendicular or parallel scattering using these modifications, it has not been possible to fit both simultaneously with the same set of parameters. This illustrates the difficulty of fitting two dimensional scattering patterns under the constraints of a physical microscopic model. It should be noted that the assumption of arm retraction does, however, qualitatively improve the fit above that obtained with no chain retraction. Even so, this observation is merely suggestive and cannot be used on its own to confirm the chain retraction process [12]. It is worth recalling that other scattering experiments [28] to test for chain retraction in linear polymers also failed to confirm the effect.

In view of the lack of available data, it is difficult to be certain of any conclusions drawn from the fitting of a single curve. However, the disagreement with the data is clear, the main feature of the scattering to explain being the large size of the correlation hole peak parallel to the stretch when compared to the perpendicular peak. The discrepancy could be due to the RPA formalism being unsuitable for the present system, or it could be due to problems in the underlying physical model. We believe the latter is far the more likely, there being several plausible criticisms of the model used. The tentative conclusion, then, is that the assumptions of the tube model, which may be sufficient to model rheological data, are not compatible with the scattering data, because scattering is a more sensitive probe of the molecular motion. The discrepancy between theory and experiment may qualitatively be explained by relaxing any one of the central assumptions of the tube model, as follows:

1. The tube path deforms affinely with the strain

This would seem to be a sensible assumption in an incompressible system where there is no free component. It has been justified by arguing that the tube diameter sets the scale below which non-affine deformations dominate. However it is known that in polymer gels, where there is a mobile component, the deformation of the network is non-affine because of local inhomogeneities in crosslink density. The mobile component allows the non-affine deformation and this leads to the observed butterfly scattering patterns [29–33] in which the scattering is enhanced parallel to the stretch. This is to be contrasted with our current understanding of "lozenge" patterns, which require only a combination of stretched and isotropic material at a given lengthscale but no centre of mass diffusion of a mobile component [23,26]. Such a combination might be produced by dangling ends in a network.

The treatment of dangling ends in our theory so far is already at a level which may be expected to produce "lozenges" (*i.e.* there is a combination of isotropic dangling end material and stretched chains within a tube). We have checked that varying the dangling-end fraction within the model is not sufficient to fit the data. We are confident that the difference between perpendicular and parallel scattering is not solely due to the same physics which gives "lozenges" in networks.

We must therefore consider whether there is any possibility of an additional "butterfly effect". There is no totally mobile component, but the dangling arm-ends do have freedom of movement within a volume which is larger than the tube diameter. The tube diameter gives the effective entanglement mesh size, so inhomogeneities in entanglement density might couple to the motion of the dangling ends. Since all the deuterated polymer is contained within the dangling ends, such a coupling would have an effect on the deuterium distribution in the system and might well enhance the scattering parallel to the stretch. To account for this possible effect would require a serious review of the above theory. The RPA calculation should include not only the quenched polymer composition distribution due to the localising tube constraints, but also a treatment of the quenched inhomogeneities in entanglement density, at the level of (say) Panyukov and Rabin's treatment of gels [29].

One feature of the "butterfly effect" is that it requires scattering contrast between the entanglement network and the mobile component. In the current H-polymer design, such contrast is possible because all the deuterium is concentrated in the dangling ends. It is possible that this effect might be eliminated (or at least reduced) by placing the deuterated blocks (say) halfway down the H-polymer arms, and contrast-matching the arm ends with the rest of the H-polymer. However, neither the theoretical nor the chemical solution to this problem seem straightforward.

2. All polymers retract by the same amount

In our derivation of structure factors for the Warner-Edwards tube model, we made the assumption that the overall extension of each tube was identical, because the tubes were long enough to sample a large spread of orientations. Whilst this may be a workable assumption in the description of the rheology, it might not be sufficient for the scattering, for the following reason. For moderately long chains of (say) 10 to 20 entanglements there is quite a large variation in tube extensions, and this variation is coupled to the orientation of the polymers. The polymers which contribute to the scattering parallel to the stretch must be (on average) more aligned in the stretch direction. Thus their tube segments also will tend to be slightly more aligned in the stretch direction, and will increase in length more than the average so that the backbones are stretched further. Thus, if branch point withdrawal occurs in some, but not all, polymers, then it will be those contributing to

the parallel scattering that will be most affected. It does not require a great deal of withdrawal to give a substantial change in the scattering, so it might require only partial withdrawal due to local cage effects at the branch points to explain the enhanced scattering parallel to the stretch. This effect may be included in the above theory without modification of the RPA formalism if scattering functions can be derived which allow explicitly for the coupling between monomer position, tube orientation and degree of retraction, without preaveraging the latter.

3. The tube diameter does not couple to the stretch

One possible model for tubes in networks [8–10,34] involves a direction-dependent tube diameter, d_μ (though we should note that the scattering formulae used in references [8,9] are highly suspect and do not involve a derivation from the microscopic network model [23,26]). Whilst the analogy in the melt tube is not obvious, it is certainly possible to use a d_μ in the above theory, and a suitable choice of coupling might be able to fit the curves. Our early attempts to use this model have indicated that the coupling between tube diameter and stretch would need to be different from that suggested for networks, and in fact would be of the form

$$d_\mu = \lambda_\mu^\nu d_0 \tag{37}$$

where ν is a *negative* power. However, we have not pursued this in detail because of the risk excessive and uncontrolled parameterisation in the model (note that all other parameters in the model could be checked against rheology values).

5 When are quenched variables important?

It is interesting to compare the scattering curves obtained in the previous section against the curves that would be obtained from a naïve application of the RPA in which quenched and annealed variables are treated at the same level (*i.e.* using Eq. (1) along with $S_{0\mathbf{q}}^{\mathrm{IJ}} = \overline{\langle \rho_{\mathbf{q}}^{\mathrm{I}} \rho_{-\mathbf{q}}^{\mathrm{J}} \rangle_0}^0$ for the structure factors). For the (simpler) triblock calculation, the difference between the "naïve" theory and the generalised RPA is less than 1% in the scattering intensity. However, Figure 7 compares the two theories for the H-polymer calculation at a stretch of $\lambda = 3$. At this strain, both theories give similar results perpendicular to the stretch, but the prediction parallel to the stretch is extremely different. At even higher strains there is a disparity both parallel and perpendicular to the stretch.

The major difference between the triblock calculation and the H-polymer calculation is the presence of the "dangling ends" from the star-like breathing modes of the H-polymer arms. The reason these "isotropic" ends are important is that in the naïve application of the RPA they are allowed to act upon the distribution of the quenched tube variables, completely washing out the large correlation hole peak parallel to the stretch. In our detailed calculation, however, the tubes are truly quenched and not affected by the isotropic dangling ends. Therefore, more of the initial melt scattering function is preserved through the quenched tube variables. We note that the result of our calculation is much closer to what would be obtained in the original RPA by constraining *all* of the H-polymer to deformed tubes. We also note that, even though our calculation failed to correctly model the experimental scattering, it is far closer than the curves obtained from the naïve application of the RPA.

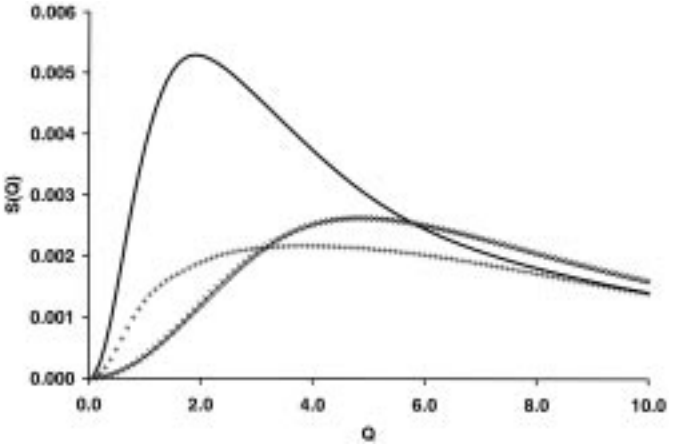

Fig. 7. Predicted scattering parallel (thick line) and perpendicular (thin line) to a stretch of $\lambda_z = 3$ from a melt of H-polymers with parameters $f_{\mathrm{A}} = 0.125$, $f_{\mathrm{cross}} = 0.346$, $f_{\mathrm{dang}} = 0.346$ and $\zeta^2 = 0.0153$. Also shown is the scattering parallel (+) and perpendicular (×) predicted by treating quenched and annealed variables at the same level.

Considerations such as this are significant when the annealed "dangling ends" and the quenched tube variables are both active at the same lengthscale so that there is interaction between them through excluded volume effects. In the triblock calculation the whole chain is confined to a tube, so whilst there are both annealed and quenched variables present, they are active at different lengthscales and do not interact to any large degree. Therefore, in that calculation it is not such a bad approximation to treat the quenched and annealed averages at the same level.

This can be summarised by saying that, in polymer systems, detailed consideration of quenched variables is vitally important when it is clear that quenched and annealed variables are inter-active at the same lengthscale.

6 Conclusions

In this paper we have shown that detailed consideration of quenched translational variables (such as might be provided by entanglements or crosslinks) is of vital importance in scattering from polymer systems with localising constraints. The difference between theories with and without proper treatment of quenched variables can be very large. We have presented a generalisation of

the Random Phase Approximation to systems with these quenched translational degrees of freedom. The extensions allowed for inclusion of correlations between quenched variables due to incompressibility. The aim was to provide a derivation of scattering patterns from microscopic models with localising constraints, so that the microscopic models can be properly tested. We demonstrated that the generalisation gave a correct treatment of the scattering in a simple example where a naïve application of the original RPA expression would fail.

We attempted to apply this theory, using the assumptions of the tube model, to a stretched melt of H-shaped polymers. It was found that the assumptions in this model were lacking in the description of the experimental scattering data. Whilst the assumption of chain retraction gave a qualitative improvement to the fit, it was impossible to confirm beyond doubt the retraction process predicted for strongly stretched melts [17]. We proposed that the lack of agreement between the microscopic model and the scattering data could be explained by relaxing any one of the central assumptions of the tube model in its original form; that the tube deforms affinely, that all polymers retract by the same degree or that the tube diameter does not couple to the stretch.

It is to be hoped that the techniques developed here will be of use in the further analysis of such experimental data. It is certain that the technique is more widely applicable. In particular, this is the correct RPA technique for the analysis of the scattering in reference [9], in which a partially deuterated triblock copolymer is crosslinked, then stretched (although modifications are necessary to account for the chain scission in that particular experiment) If the correct RPA technique is used, then comparisons between different microscopic models (*e.g.* tube potentials coupling in different ways to the stretch) are then valid.

I would like to thank all those involved in reference [12] for aspects of work related to this paper. In particular I thank T.C.B. McLeish for suggesting the task (and for helpful comments regarding this manuscript), J. Allgaier and R.N. Young for making the H-polymer and R.K. Heenan for overseeing the neutron scattering experiment. I also thank M.G. Brereton and W. Pyckhout-Hintzen for useful discussions.

Appendix A: RPA with quenched variables

In this appendix we provide details of the generalisation of the Random Phase Approximation (RPA) to deal with quenched variables. The RPA deals with the statistical mechanics of concentration fluctuations in polymer systems. To proceed with the RPA it is necessary to calculate the first and second moment averages of the density variables $\rho_{\mathbf{q}}^{\mathrm{A}}$ and $\rho_{\mathbf{q}}^{\mathrm{B}}$. In the usual application of the RPA to a melt we find;

$$\begin{aligned} \langle \rho_{\mathbf{q}} \rangle &= 0 \\ \langle \rho_{\mathbf{q}} \rho_{-\mathbf{k}} \rangle &= 0 \quad \text{for } \mathbf{q} \neq \mathbf{k}. \end{aligned} \tag{A.1}$$

This is due to the translational symmetry of the system (the chains are free to move anywhere). Thus the usual RPA is concerned only with second moment averages of the form $\langle |\rho_{\mathbf{q}}|^2 \rangle$. However, if the chains are localised (*i.e.* their translational degrees of freedom are quenched, as in a network) then the averages must be calculated subject to this constraint. The translational symmetry is destroyed and $\langle \rho_{\mathbf{q}} \rangle$ and $\langle \rho_{\mathbf{q}} \rho_{-\mathbf{k}} \rangle$ are non-zero. Hence, the standard RPA calculation is not possible for networks and other systems with quenched translational degrees of freedom. In an earlier paper [20] we demonstrated that it is possible to extend the standard RPA method by using generalised Gaussian functions which account of the non-zero mean $\langle \rho_{\mathbf{q}} \rangle$ and correlation $\langle \rho_{\mathbf{q}} \rho_{-\mathbf{k}} \rangle$. The chain constraints can be explicitly fixed throughout the main part of the calculation, so that their effect on the interactions in the system is retained. Importantly, the non-zero mean $\langle \rho_{\mathbf{q}} \rangle$ acts to give "frozen-in" composition fluctuations which significantly affect the temperature variation of the scattering profile. At the end of the calculation we averaged over the quenched constraints. The quenched variable average, denoted by $\overline{(\dots)}$, restores translational symmetry so that

$$\begin{aligned} \overline{\langle \rho_{\mathbf{q}} \rangle} &= 0 \\ \overline{\langle \rho_{\mathbf{q}} \rho_{-\mathbf{k}} \rangle} &= 0 \quad \text{for } \mathbf{q} \neq \mathbf{k} \end{aligned} \tag{A.2}$$

and only two types of second-order correlation function survive. These are $\overline{|\langle \rho_{\mathbf{q}} \rangle|^2}$ (related to the mean of the concentration fluctuations) and $\overline{\langle |\rho_{\mathbf{q}}|^2 \rangle - |\langle \rho_{\mathbf{q}} \rangle|^2}$ (related to fluctuations about this mean).

The main deficiency of the calculation in our paper [20] was that it did not allow for chain-chain correlations in the quenched variables, or any other statistical correlations between the A and B monomers (such as would be present in block copolymers like the H-shaped polymer of Fig. 1). We now calculate a more general result that accounts for these effects.

To perform the calculation, we use a method due to Ohta and Kawasaki [35]. The method allows the derivation of a mean-field free energy functional to arbitrary order in the density variables, $\rho_{\mathbf{q}}$, though we shall expand only to second order. The method has been used extensively by authors such as Fredrickson, Milner and Leibler in calculations for block copolymers (see *e.g.* [36]). We shall adapt the method to include the essential physics arising from the localisation of chains in tubes.

The partition function for an interacting blend of polymers may be written in the form

$$Z = \left\langle \exp\left(-U\left\{\rho_{\mathbf{q}}^{\mathrm{A}}, \rho_{\mathbf{q}}^{\mathrm{B}}\right\}\right)\right\rangle_0 \tag{A.3}$$

where $\langle \dots \rangle_0$ represents an average over the chain configurations in the non-interacting limit (analogous to a sum over the microstates of the system). This average is taken subject to the localising constraints being quenched (or fixed). The intention is to calculate the statistical mechanics with these constraints fixed, and to average over them at the end of the calculation. $U\left\{\rho_{\mathbf{q}}^{\mathrm{A}}, \rho_{\mathbf{q}}^{\mathrm{B}}\right\}$ is the internal energy (in units of $k_{\mathrm{B}}T$) due to monomer-monomer

interactions. We write this as

$$U\left\{\rho_{\mathbf{q}}^{\mathrm{A}},\rho_{\mathbf{q}}^{\mathrm{B}}\right\}=\frac{1}{2\Omega}\sum_{\mathbf{q}}\left\{V\left|\rho_{\mathbf{q}}^{\mathrm{A}}+\rho_{\mathbf{q}}^{\mathrm{B}}\right|^{2}-\frac{2\chi}{\rho}\left|\rho_{\mathbf{q}}^{\mathrm{A}}\right|^{2}\right\} \tag{A.4}$$

where Ω is the system volume, ρ is the mean monomer density and χ is the Flory interaction parameter. At the end of the calculation we shall take the limit $V\rightarrow\infty$ to enforce incompressibility.

We proceed by introducing the auxiliary density order parameters $P_{\mathbf{q}}^{\mathrm{A}}$ and $P_{\mathbf{q}}^{\mathrm{B}}$ *via* delta functions, so that

$$\begin{aligned}Z&=\left\langle\int\left(\prod_{\mathbf{q}}\mathrm{d}P_{\mathbf{q}}^{\mathrm{A}}\mathrm{d}P_{\mathbf{q}}^{\mathrm{B}}\right)\right.\\&\left.\times\prod_{\mathbf{q}}\delta\left(\rho_{\mathbf{q}}^{\mathrm{A}}-P_{\mathbf{q}}^{\mathrm{A}}\right)\delta\left(\rho_{\mathbf{q}}^{\mathrm{B}}-P_{\mathbf{q}}^{\mathrm{B}}\right)\exp\left(-U\left\{\rho_{\mathbf{q}}^{\mathrm{A}},\rho_{\mathbf{q}}^{\mathrm{B}}\right\}\right)\right\rangle_{0}\\&=\int\left(\prod_{\mathbf{q}}\mathrm{d}P_{\mathbf{q}}^{\mathrm{A}}\mathrm{d}P_{\mathbf{q}}^{\mathrm{B}}\right)\exp\left(-U\left\{P_{\mathbf{q}}^{\mathrm{A}},P_{\mathbf{q}}^{\mathrm{B}}\right\}\right)R\left\{P_{\mathbf{q}}^{\mathrm{A}},P_{\mathbf{q}}^{\mathrm{B}}\right\}\end{aligned} \tag{A.5}$$

where

$$R\left\{P_{\mathbf{q}}^{\mathrm{A}},P_{\mathbf{q}}^{\mathrm{B}}\right\}=\left\langle\prod_{\mathbf{q}}\delta\left(\rho_{\mathbf{q}}^{\mathrm{A}}-P_{\mathbf{q}}^{\mathrm{A}}\right)\delta\left(\rho_{\mathbf{q}}^{\mathrm{B}}-P_{\mathbf{q}}^{\mathrm{B}}\right)\right\rangle_{0}.$$

If $R\left\{P_{\mathbf{q}}^{\mathrm{A}},P_{\mathbf{q}}^{\mathrm{B}}\right\}$ is calculated, then this will yield a free energy functional in the order parameters $P_{\mathbf{q}}^{\mathrm{A}}$ and $P_{\mathbf{q}}^{\mathrm{B}}$, since by comparison with

$$Z=\int\left(\prod_{\mathbf{q}}\mathrm{d}P_{\mathbf{q}}^{\mathrm{A}}\mathrm{d}P_{\mathbf{q}}^{\mathrm{B}}\right)\exp\left(-F\left\{P_{\mathbf{q}}^{\mathrm{A}},P_{\mathbf{q}}^{\mathrm{B}}\right\}\right) \tag{A.6}$$

we see that

$$F\left\{P_{\mathbf{q}}^{\mathrm{A}},P_{\mathbf{q}}^{\mathrm{B}}\right\}=U\left\{P_{\mathbf{q}}^{\mathrm{A}},P_{\mathbf{q}}^{\mathrm{B}}\right\}-\ln\left(R\left\{P_{\mathbf{q}}^{\mathrm{A}},P_{\mathbf{q}}^{\mathrm{B}}\right\}\right). \tag{A.7}$$

Calculation of $R\left\{P_{\mathbf{q}}^{\mathrm{A}},P_{\mathbf{q}}^{\mathrm{B}}\right\}$ proceeds by exponentiating the delta-functions to give

$$\begin{aligned}R\left\{P_{\mathbf{q}}^{\mathrm{A}},P_{\mathbf{q}}^{\mathrm{B}}\right\}&=\left\langle\int\left(\prod_{\mathbf{q}}\mathrm{d}J_{\mathbf{q}}^{\mathrm{A}}\mathrm{d}J_{\mathbf{q}}^{\mathrm{B}}\right)\right.\\&\left.\times\exp\left(\mathrm{i}\sum_{\mathbf{q}}J_{\mathbf{q}}^{\mathrm{A}}\left(\rho_{\mathbf{q}}^{\mathrm{A}}-P_{\mathbf{q}}^{\mathrm{A}}\right)+J_{\mathbf{q}}^{\mathrm{B}}\left(\rho_{\mathbf{q}}^{\mathrm{B}}-P_{\mathbf{q}}^{\mathrm{B}}\right)\right)\right\rangle_{0}\\&=\int\left(\prod_{\mathbf{q}}\mathrm{d}J_{\mathbf{q}}^{\mathrm{A}}dJ_{\mathbf{q}}^{\mathrm{B}}\right)\exp\left(-\mathrm{i}\sum_{\mathbf{q}}\left(J_{\mathbf{q}}^{\mathrm{A}}P_{\mathbf{q}}^{\mathrm{A}}+J_{\mathbf{q}}^{\mathrm{B}}P_{\mathbf{q}}^{\mathrm{B}}\right)+G\right)\end{aligned} \tag{A.8}$$

where

$$G=\ln\left\langle\exp\left(\mathrm{i}\sum_{\mathbf{q}}J_{\mathbf{q}}^{\mathrm{A}}\rho_{\mathbf{q}}^{\mathrm{A}}+J_{\mathbf{q}}^{\mathrm{B}}\rho_{\mathbf{q}}^{\mathrm{B}}\right)\right\rangle_{0}. \tag{A.9}$$

A mean-field free energy functional to nth order in the density variables is obtained by expanding G to nth order in the variables $J_{\mathbf{q}}^{\mathrm{A}}$ and $J_{\mathbf{q}}^{\mathrm{B}}$, then performing the integration over them by the saddle point method. We expand G to second order;

$$\begin{aligned}G=&\,\mathrm{i}\sum_{\mathbf{q}}J_{\mathbf{q}}^{\mathrm{A}}\left\langle\rho_{\mathbf{q}}^{\mathrm{A}}\right\rangle_{0}+J_{\mathbf{q}}^{\mathrm{B}}\left\langle\rho_{\mathbf{q}}^{\mathrm{B}}\right\rangle_{0}\\&-\frac{1}{2!}\sum_{\mathbf{q}_1,\mathbf{q}_2}\left\{\begin{array}{c}J_{\mathbf{q}_1}^{\mathrm{A}}J_{\mathbf{q}_2}^{\mathrm{A}}\left(\left\langle\rho_{\mathbf{q}_1}^{\mathrm{A}}\rho_{\mathbf{q}_2}^{\mathrm{A}}\right\rangle_{0}-\left\langle\rho_{\mathbf{q}_1}^{\mathrm{A}}\right\rangle_{0}\left\langle\rho_{\mathbf{q}_2}^{\mathrm{A}}\right\rangle_{0}\right)\\+J_{\mathbf{q}_1}^{\mathrm{B}}J_{\mathbf{q}_2}^{\mathrm{B}}\left(\left\langle\rho_{\mathbf{q}_1}^{\mathrm{B}}\rho_{\mathbf{q}_2}^{\mathrm{B}}\right\rangle_{0}-\left\langle\rho_{\mathbf{q}_1}^{\mathrm{B}}\right\rangle_{0}\left\langle\rho_{\mathbf{q}_2}^{\mathrm{B}}\right\rangle_{0}\right)\\+2J_{\mathbf{q}_1}^{\mathrm{A}}J_{\mathbf{q}_2}^{\mathrm{B}}\left(\left\langle\rho_{\mathbf{q}_1}^{\mathrm{A}}\rho_{\mathbf{q}_2}^{\mathrm{B}}\right\rangle_{0}-\left\langle\rho_{\mathbf{q}_1}^{\mathrm{A}}\right\rangle_{0}\left\langle\rho_{\mathbf{q}_2}^{\mathrm{B}}\right\rangle_{0}\right)\end{array}\right\}\\&+O\left(J^{3}\right).\end{aligned} \tag{A.10}$$

Notice that in the calculation for a melt, as in reference [36], many of these terms vanish because translational symmetry implies that quantities such as $\left\langle\rho_{\mathbf{q}}^{\mathrm{A}}\right\rangle_{0}$ are zero. Performing the quenched average restores the melt symmetry, so we see that pre-averaging all the structure factors at this stage would miss some of the important physics, in particular the effect of frozen-in fluctuations. However, we are able to use insights gained from the calculation in our paper [20] to simplify the present calculation.

Suppose the total number of chains[1] in the system is n. We note that structure factors such as $\left\langle\rho_{\mathbf{q}_1}^{\mathrm{A}}\rho_{\mathbf{q}_2}^{\mathrm{A}}\right\rangle_{0}$ involve a sum over a large number of chains and will thus be typically close to their quenched average value. Under the quenched average, each chain is independent and so the quenched average scales as n, whilst the typical deviation from the quenched average is of order $n^{\frac{1}{2}}$. Importantly, for any given system, the deviation from the quenched average is a fixed quantity. In the first-order terms of (A.10) this deviation is not negligible because the quenched averages such as $\overline{\left\langle\rho_{\mathbf{q}}^{\mathrm{A}}\right\rangle_{0}}$ are strictly zero. Thus we cannot pre-average the first order terms.

However, the quenched average of the second order terms is not strictly zero, and we can write

$$\begin{aligned}&\left\langle\rho_{\mathbf{q}_1}^{\mathrm{A}}\rho_{\mathbf{q}_2}^{\mathrm{A}}\right\rangle_{0}-\left\langle\rho_{\mathbf{q}_1}^{\mathrm{A}}\right\rangle_{0}\left\langle\rho_{\mathbf{q}_2}^{\mathrm{A}}\right\rangle_{0}\simeq\\&\qquad\overline{\left\langle\rho_{\mathbf{q}_1}^{\mathrm{A}}\rho_{\mathbf{q}_1}^{\mathrm{A}}\right\rangle_{0}-\left\langle\rho_{\mathbf{q}_1}^{\mathrm{A}}\right\rangle_{0}\left\langle\rho_{\mathbf{q}_1}^{\mathrm{A}}\right\rangle_{0}}\delta_{\mathbf{q}_1+\mathbf{q}_2}+O\left(n^{\frac{1}{2}}\right)\end{aligned} \tag{A.11}$$

The pre-averaging is valid here because the leading term is of order n. In the calculation of the scattering structure factor, which requires only a second order free energy expansion, this term dominates and we can neglect the order $n^{\frac{1}{2}}$ deviations. It is worth commenting that the deviations will be significant and should be included in any calculation involving higher order terms in the free energy.

[1] In the context of networks, to avoid loss of generality, we define a "chain" to be one of the starting units used to create the network. The "quenched average" is then an average over all possible combinations of the "chains" and is to some extent analogous to a melt average over the uncrosslinked system.

$$F\left\{\rho_{\mathbf{q}}\right\}=\frac{1}{2}\sum_{\mathbf{q}}\left\{\frac{T_{\mathbf{q}}^{\mathrm{BB}}\left|\rho_{\mathbf{q}}-d_{\mathbf{q}}^{\mathrm{A}}\right|^{2}+T_{\mathbf{q}}^{\mathrm{AA}}\left|\rho_{\mathbf{q}}+d_{\mathbf{q}}^{\mathrm{B}}\right|^{2}+2T_{\mathbf{q}}^{\mathrm{AB}}\left(\rho_{\mathbf{q}}-d_{\mathbf{q}}^{\mathrm{A}}\right)\left(\rho_{-\mathbf{q}}+d_{-\mathbf{q}}^{\mathrm{B}}\right)}{T_{\mathbf{q}}^{\mathrm{AA}}T_{\mathbf{q}}^{\mathrm{BB}}-\left(T_{\mathbf{q}}^{\mathrm{AB}}\right)^{2}}-\frac{2\chi}{\Omega\rho}\left|\rho_{\mathbf{q}}\right|^{2}\right\}. \tag{A.14}$$

$$S\left(\mathbf{q}\right)=\overline{\left\langle\left|\rho_{\mathbf{q}}\right|^{2}\right\rangle}=\frac{1}{\left(T_{\mathrm{inc}}^{-1}-\frac{2\chi}{\Omega\rho}\right)}+\frac{\Delta_{\mathbf{q}}^{\mathrm{AA}}\left(T_{\mathbf{q}}^{\mathrm{BB}}+T_{\mathbf{q}}^{\mathrm{AB}}\right)^{2}+\Delta_{\mathbf{q}}^{\mathrm{BB}}\left(T_{\mathbf{q}}^{\mathrm{AA}}+T_{\mathbf{q}}^{\mathrm{AB}}\right)^{2}-2\Delta_{\mathbf{q}}^{\mathrm{AB}}\left(T_{\mathbf{q}}^{\mathrm{AA}}+T_{\mathbf{q}}^{\mathrm{AB}}\right)\left(T_{\mathbf{q}}^{\mathrm{BB}}+T_{\mathbf{q}}^{\mathrm{AB}}\right)}{\left(T_{\mathrm{inc}}^{-1}-\frac{2\chi}{\Omega\rho}\right)^{2}\left(T_{\mathbf{q}}^{\mathrm{AA}}T_{\mathbf{q}}^{\mathrm{BB}}-\left(T_{\mathbf{q}}^{\mathrm{AB}}\right)^{2}\right)^{2}} \tag{A.15}$$

Making the pre-averaging approximation on the second-order terms allows us to write

$$\begin{aligned}G=\sum_{\mathbf{q}}\Big\{&\mathrm{i}\left(J_{\mathbf{q}}^{\mathrm{A}}d_{\mathbf{q}}^{\mathrm{A}}+J_{\mathbf{q}}^{\mathrm{B}}d_{\mathbf{q}}^{\mathrm{B}}\right)\\&-\frac{1}{2!}\left(J_{\mathbf{q}}^{\mathrm{A}}J_{-\mathbf{q}}^{\mathrm{A}}T_{\mathbf{q}}^{\mathrm{AA}}+J_{\mathbf{q}}^{\mathrm{B}}J_{-\mathbf{q}}^{\mathrm{B}}T_{\mathbf{q}}^{\mathrm{BB}}+2J_{\mathbf{q}}^{\mathrm{A}}J_{-\mathbf{q}}^{\mathrm{B}}T_{\mathbf{q}}^{\mathrm{AB}}\right)\Big\}\\&+O\left(J^{3},J^{2}n^{\frac{1}{2}}\right)\end{aligned} \tag{A.12}$$

where

$$\begin{aligned}d_{\mathbf{q}}^{\mathrm{I}}&=\left\langle\rho_{\mathbf{q}}^{\mathrm{I}}\right\rangle_{0}\\T_{\mathbf{q}}^{\mathrm{IJ}}&=\overline{\left\langle\rho_{\mathbf{q}}^{\mathrm{I}}\rho_{-\mathbf{q}}^{\mathrm{J}}\right\rangle_{0}-\left\langle\rho_{\mathbf{q}}^{\mathrm{I}}\right\rangle_{0}\left\langle\rho_{-\mathbf{q}}^{\mathrm{J}}\right\rangle_{0}}\,.\end{aligned}$$

The saddle point integration to obtain $R\left\{P_{\mathbf{q}}^{\mathrm{A}},P_{\mathbf{q}}^{\mathrm{B}}\right\}$ in equation (A.8) is now straightforward. If we also take the limit $V\rightarrow\infty$ and integrate out $P_{\mathbf{q}}^{\mathrm{B}}$ (setting $P_{\mathbf{q}}^{\mathrm{A}}=-P_{\mathbf{q}}^{\mathrm{B}}=\rho_{\mathbf{q}}$) we obtain a final expression for the partition function

$$Z=\int\left(\prod_{\mathbf{q}}\mathrm{d}\rho_{\mathbf{q}}\right)\exp\left(-F\left\{\rho_{\mathbf{q}}\right\}\right) \tag{A.13}$$

where the free energy functional $F\left\{\rho_{\mathbf{q}}\right\}$ is given by

see equation (A.14) above.

This expression implies Gaussian fluctuations about a non-zero mean. The non-zero mean is related to the "frozen-in" quenched average densities $d_{\mathbf{q}}^{\mathrm{A}}$ and $d_{\mathbf{q}}^{\mathrm{B}}$. As in reference [20] we calculate this mean and the size of the fluctuations about it to give the structure factor. Taking the quenched average of the structure factor gives

see equation (A.15) above

where

$$T_{\mathrm{inc}}=\frac{T_{\mathbf{q}}^{\mathrm{AA}}T_{\mathbf{q}}^{\mathrm{BB}}-\left(T_{\mathbf{q}}^{\mathrm{AB}}\right)^{2}}{T_{\mathbf{q}}^{\mathrm{AA}}+T_{\mathbf{q}}^{\mathrm{BB}}+2T_{\mathbf{q}}^{\mathrm{AB}}} \tag{A.16}$$

and

$$\Delta_{\mathbf{q}}^{\mathrm{IJ}}=\overline{\left\langle\rho_{\mathbf{q}}^{\mathrm{I}}\right\rangle_{0}\left\langle\rho_{-\mathbf{q}}^{\mathrm{J}}\right\rangle_{0}}. \tag{A.17}$$

The equation (A.15) is the central result of this Appendix. The first term in $S\left(\mathbf{q}\right)$ arises from fluctuations about a non-zero mean. The second term is due to this mean. It is possible to use a microscopic molecular model to obtain expressions for the structure factors $\Delta_{\mathbf{q}}^{\mathrm{IJ}}$ and $T_{\mathbf{q}}^{\mathrm{IJ}}$ and thus to make quantitative comparison with experiment. In particular, the "frozen-in" fluctuations are well defined through the structure factors $\Delta_{\mathbf{q}}^{\mathrm{IJ}}$. In the limit $\chi=0$, the equation (A.15) reduces to (5).

Appendix B: Accounting for tube-tube correlations

In this Appendix we consider how to account for correlations between quenched variables which are brought about by incompressibility constraints. There are two types of structure factor which must be calculated in equation (5). The first is of type

$$T_{\mathbf{q}}^{\mathrm{IJ}}=\overline{\left\langle\rho_{\mathbf{q}}^{\mathrm{I}}\rho_{-\mathbf{q}}^{\mathrm{J}}\right\rangle_{0}-\left\langle\rho_{\mathbf{q}}^{\mathrm{I}}\right\rangle_{0}\left\langle\rho_{-\mathbf{q}}^{\mathrm{J}}\right\rangle_{0}}^{\mathrm{inc}} \tag{B.1}$$

which is related to fluctuations about the mean of the frozen-in concentration fluctuations. The annealed average $\left\langle\ldots\right\rangle_{0}$ is calculated subject to quenched tube variables but with the chains not otherwise interacting. The quenched average $\overline{\left(\ldots\right)}^{\mathrm{inc}}$ must account for correlations between tubes due to incompressibility, and this is denoted by the superscript "inc". The second type of structure factor is of type

$$\Delta_{\mathbf{q}}^{\mathrm{IJ}}=\overline{\left\langle\rho_{\mathbf{q}}^{\mathrm{I}}\right\rangle_{0}\left\langle\rho_{-\mathbf{q}}^{\mathrm{J}}\right\rangle_{0}}^{\mathrm{inc}} \tag{B.2}$$

and this is related to the non-zero mean of the concentration profile. It is convenient also to define the equivalent structure factors in the absence of tube-tube correlations

$$\begin{aligned}T_{0\mathbf{q}}^{\mathrm{IJ}}&=\overline{\left\langle\rho_{\mathbf{q}}^{\mathrm{I}}\rho_{-\mathbf{q}}^{\mathrm{J}}\right\rangle_{0}-\left\langle\rho_{\mathbf{q}}^{\mathrm{I}}\right\rangle_{0}\left\langle\rho_{-\mathbf{q}}^{\mathrm{J}}\right\rangle_{0}}^{0}\\\Delta_{0\mathbf{q}}^{\mathrm{IJ}}&=\overline{\left\langle\rho_{\mathbf{q}}^{\mathrm{I}}\right\rangle_{0}\left\langle\rho_{-\mathbf{q}}^{\mathrm{J}}\right\rangle_{0}}^{0}\end{aligned} \tag{B.3}$$

where the superscript 0 denotes the absence of interactions in the quenched average. In these structure factors there are no correlations between chains or tubes, so the results are simply proportional to the single chain structure factors which may be obtained from a model such as

the Warner-Edwards model (with proportionality factor n, the number of chains).

Since, under the annealed average, $\langle \dots \rangle_0$, chains are independent, we find that for two different chains ($\alpha \neq \alpha'$);

$$\left\langle \rho_{\mathbf{q}}^{\mathrm{I}\alpha} \rho_{-\mathbf{q}}^{\mathrm{J}\alpha'} \right\rangle_0 = \left\langle \rho_{\mathbf{q}}^{\mathrm{I}\alpha} \right\rangle_0 \left\langle \rho_{-\mathbf{q}}^{\mathrm{J}\alpha'} \right\rangle_0 \tag{B.4}$$

and so the contribution to both $T_{\mathbf{q}}^{\mathrm{IJ}}$ and $T_{0\mathbf{q}}^{\mathrm{IJ}}$ from separate chains is zero. The only contribution to these is from the single chain structure factors. In an incompressible melt, the chain configurations are Gaussian, so the excluded volume interactions have no effect on the single chain structure factors and we conclude that

$$T_{\mathbf{q}}^{\mathrm{IJ}} = T_{0\mathbf{q}}^{\mathrm{IJ}}. \tag{B.5}$$

We can thus obtain structure factors of form $T_{\mathbf{q}}^{\mathrm{IJ}}$ directly from a microscopic model for the chain and ignore the incompressibility effect.

The situation is not so simple for the structure factors of type $\Delta_{\mathbf{q}}^{\mathrm{IJ}}$. When there are tube-tube correlations, the contribution to $\Delta_{\mathbf{q}}^{\mathrm{IJ}}$ from separate chains is non-zero, whilst $\Delta_{0\mathbf{q}}^{\mathrm{AIJ}}$ contains only the single chain structure factors. Consequently

$$\Delta_{\mathbf{q}}^{\mathrm{IJ}} \neq \Delta_{0\mathbf{q}}^{\mathrm{IJ}} \tag{B.6}$$

and it is necessary to account for chain-chain correlations.

To achieve this, we must examine the chain configurations both before and after the stretch. After the stretch the position of monomer l on chain α is $\mathbf{r}_l^\alpha$, and we use

$$\begin{aligned} \rho_{\mathbf{q}}^{\mathrm{A}} &= \sum_{\alpha,l} y_l^\alpha \exp\left(\mathrm{i}\mathbf{q}\cdot\mathbf{r}_l^\alpha\right) \\ \rho_{\mathbf{q}}^{\mathrm{B}} &= \sum_{\alpha,l} (1-y_l^\alpha) \exp\left(\mathrm{i}\mathbf{q}\cdot\mathbf{r}_l^\alpha\right). \end{aligned} \tag{B.7}$$

We make the further definitions that the position of monomer l on chain α *before* the stretch is $\mathbf{x}_l^\alpha$ and we define the total monomer density

$$\varphi_{\mathbf{q}} = \sum_{\alpha,l} \exp\left(\mathrm{i}\mathbf{q}\cdot\mathbf{E}\cdot\mathbf{x}_l^\alpha\right) \tag{B.8}$$

Notice that the sum in $\varphi_{\mathbf{q}}$ is over all A and B monomers. We include the strain matrix $\mathbf{E}$ in this definition to bring the $\mathbf{x}_l^\alpha$ into the same space as the $\mathbf{r}_l^\alpha$, thus avoiding problems with translational symmetry in later averages.

Since the tube variables are slow, there are correlations between the $\mathbf{x}_l^\alpha$ and the $\mathbf{r}_l^\alpha$ because they are confined to the same tubes. To account for incompressibility before the stretch, we must perform the necessary averaging over all $\{\mathbf{x}_l^\alpha, \mathbf{r}_l^\alpha\}$ configurations, but eliminate all those configurations which do not satisfy incompressibility in the $\{\mathbf{x}_l^\alpha\}$ space. As we shall see, the RPA formalism allows this calculation to be performed.

To calculate the $\Delta_{\mathbf{q}}^{\mathrm{IJ}}$ we perform an RPA calculation on the order parameter fields $\left\langle \rho_{\mathbf{q}}^{\mathrm{A}} \right\rangle_0$, $\left\langle \rho_{\mathbf{q}}^{\mathrm{B}} \right\rangle_0$ and $\varphi_{\mathbf{q}}$. We seek to calculate correlation functions between these fields, firstly subject to a completely free distribution of the $\{\mathbf{x}_l^\alpha, \mathbf{r}_l^\alpha\}$, and subsequently enforcing incompressibility in the $\{\mathbf{x}_l^\alpha\}$. We separate out the averages over the slow tube variables and the fast variables for fluctuations within the tube. The averages over the fast variables in the $\{\mathbf{r}_l^\alpha\}$ and $\{\mathbf{x}_l^\alpha\}$ are calculated subject to them being confined to the same tubes and we denote these averages (in the absence of interactions) by $\langle \dots \rangle_0$ for the $\{\mathbf{r}_l^\alpha\}$. In the absence of tube-tube correlations, the bare correlation functions are

$$\begin{aligned} \Delta_{0\mathbf{q}}^{\mathrm{IJ}} &= \overline{\left\langle \rho_{\mathbf{q}}^{\mathrm{I}} \right\rangle_0 \left\langle \rho_{-\mathbf{q}}^{\mathrm{J}} \right\rangle_0}^0 \\ T_{0\mathbf{q}}^{\mathrm{IJ}} &= \overline{\left\langle \rho_{\mathbf{q}}^{\mathrm{I}} \rho_{-\mathbf{q}}^{\mathrm{J}} \right\rangle_0 - \left\langle \rho_{\mathbf{q}}^{\mathrm{I}} \right\rangle_0 \left\langle \rho_{-\mathbf{q}}^{\mathrm{J}} \right\rangle_0}^0 \\ D_{\mathbf{q}}^{\mathrm{I}} &= \overline{\left\langle \rho_{\mathbf{q}}^{\mathrm{I}} \right\rangle_0 \left\langle \varphi_{-\mathbf{q}} \right\rangle_0}^0 \\ S_{\mathbf{q}}^{\mathrm{tot}} &= \overline{\left\langle \varphi_{\mathbf{q}} \varphi_{-\mathbf{q}} \right\rangle_0}^0. \end{aligned} \tag{B.9}$$

These are calculated subject to a free distribution of $\{\mathbf{x}_l^\alpha, \mathbf{r}_l^\alpha\}$ and are all proportional to single chain correlation functions calculable from a microscopic model such as the Warner-Edwards model.

Since we are dealing with a large number of chains, the fields $\left\langle \rho_{\mathbf{q}}^{\mathrm{A}} \right\rangle_0$, $\left\langle \rho_{\mathbf{q}}^{\mathrm{B}} \right\rangle_0$ and $\varphi_{\mathbf{q}}$ involve a sum over a large number of variables and are thus, to good approximation, Gaussian. The probability distribution of the fields in the absence of interactions is

$$P\left\{\left\langle \rho_{\mathbf{q}}^{\mathrm{A}} \right\rangle_0, \left\langle \rho_{\mathbf{q}}^{\mathrm{B}} \right\rangle_0, \varphi_{\mathbf{q}}\right\} \sim \exp\left[-\tfrac{1}{2}\sum_{\mathbf{q}} \left(\left\langle \rho_{-\mathbf{q}}^{\mathrm{A}} \right\rangle_0 \left\langle \rho_{-\mathbf{q}}^{\mathrm{B}} \right\rangle_0 \varphi_{-\mathbf{q}} \right) \cdot \mathbf{M}^{-1} \cdot \begin{pmatrix} \left\langle \rho_{\mathbf{q}}^{\mathrm{A}} \right\rangle_0 \\ \left\langle \rho_{\mathbf{q}}^{\mathrm{B}} \right\rangle_0 \\ \varphi_{\mathbf{q}} \end{pmatrix}\right] \tag{B.10}$$

where $\mathbf{M}$ is the matrix of correlation functions:

$$\mathbf{M} = \begin{bmatrix} \Delta_{0\mathbf{q}}^{\mathrm{AA}} & \Delta_{0\mathbf{q}}^{\mathrm{AB}} & D_{\mathbf{q}}^{\mathrm{A}} \\ \Delta_{0\mathbf{q}}^{\mathrm{AB}} & \Delta_{0\mathbf{q}}^{\mathrm{BB}} & D_{\mathbf{q}}^{\mathrm{B}} \\ D_{\mathbf{q}}^{\mathrm{A}} & D_{\mathbf{q}}^{\mathrm{B}} & S_{\mathbf{q}}^{\mathrm{tot}} \end{bmatrix}. \tag{B.11}$$

Incompressibility in the melt prior to stretching may now be introduced, by noting that this interaction couples with the variable $\varphi_{\mathbf{q}}$, which is the total density of monomers prior to the stretch. Using the interaction matrix

$$\mathbf{V} = \begin{bmatrix} 0 & 0 & 0 \\ 0 & 0 & 0 \\ 0 & 0 & V \end{bmatrix} \tag{B.12}$$

and following the standard RPA calculation, the probability distribution of the chosen fields is modified by a Boltzmann factor and becomes identical to equation (B.10) but with $\mathbf{M}^{-1}$ replaced by $\mathbf{M}^{-1} + \mathbf{V}$. Incompressibility is enforced by taking the limit $V \to \infty$. The correlation functions, in the presence of the $\{\mathbf{x}_l^\alpha\}$ incompressibility, are then contained in the inverse matrix $\left(\mathbf{M}^{-1} + \mathbf{V}\right)^{-1}$ and

are found to be

$$\Delta^{\rm IJ}_{\mathbf{q}} = \Delta^{\rm IJ}_{0\mathbf{q}} - \frac{D^{\rm I}_{\mathbf{q}} D^{\rm J}_{\mathbf{q}}}{S^{\rm tot}_{\mathbf{q}}} \,. \qquad \text{(B.13)}$$

In summary, a full derivation of the structure factor using equation (5) requires not only the calculation of the single chain structure factors $\Delta^{\rm IJ}_{0\mathbf{q}}$ and $T^{\rm IJ}_{0\mathbf{q}}$ but also corrections to be made for correlations between tubes. These corrections require calculation of the single chain correlation functions $D^{\rm A}_{\mathbf{q}}$ and $D^{\rm B}_{\mathbf{q}}$ between chains in the same tube before and after stretching and also of the total structure factor $S^{\rm tot}_{\mathbf{q}}$ of the melt before stretching.

Appendix C: Scattering function for blends of identical chains with quenched variables

In a recent paper [23] we calculated the scattering function for a partially labelled network, using the model of a stretched chain with "dangling ends". We calculated the "bare" scattering function (with the dangling ends taken to be isotropic) and stated that this was the correct expression for the total scattering if the network consisted of identical chains, some of which were labelled. This statement may be proven using the results derived in this paper for the RPA in the presence of quenched variables. In equations (5, 9) we have expressions for the scattering intensity. If the system contains only chains of type A and B, which are labelled differently but otherwise identical, then these equations may be greatly simplified, because the single chain structure factors are the same for the A and B chains. Ignoring prefactors common to all the structure factors we can write

$$\begin{array}{ccc} T^{\rm AA}_{\mathbf{q}} = \phi_{\rm A} T_{\mathbf{q}} & T^{\rm BB}_{\mathbf{q}} = \phi_{\rm B} T_{\mathbf{q}} & T^{\rm AB}_{\mathbf{q}} = 0 \\ \Delta^{\rm AA}_{0\mathbf{q}} = \phi_{\rm A} \Delta_{0\mathbf{q}} & \Delta^{\rm BB}_{0\mathbf{q}} = \phi_{\rm B} \Delta_{0\mathbf{q}} & \Delta^{\rm AB}_{0\mathbf{q}} = 0 \\ D^{\rm A}_{\mathbf{q}} = \phi_{\rm A} D_{\mathbf{q}} & D^{\rm B}_{\mathbf{q}} = \phi_{\rm B} D_{\mathbf{q}} & \end{array}$$

where $\phi_{\rm A}$ and $\phi_{\rm B} = 1 - \phi_{\rm A}$ are the volume fractions of the A and B components respectively. Substituting these into equations (5, 9) gives

$$\begin{aligned} I(\mathbf{q}) &= \frac{\phi_{\rm A}\phi_{\rm B} T^2_{\mathbf{q}}}{T_{\mathbf{q}}} \\ &+ \frac{\phi_{\rm A}\phi_{\rm B}^2 \Delta_{0\mathbf{q}} T^2_{\mathbf{q}} + \phi_{\rm A}^2 \phi_{\rm B} \Delta_{0\mathbf{q}} T^2_{\mathbf{q}} - \left(S^{\rm tot}_{\mathbf{q}}\right)^{-1} \left(D^{\rm A}_{\mathbf{q}} T^{\rm BB}_{\mathbf{q}} - D^{\rm B}_{\mathbf{q}} T^{\rm AA}_{\mathbf{q}}\right)^2}{T^2_{\mathbf{q}}} \\ &= \phi_{\rm A}\phi_{\rm B} \left(T_{\mathbf{q}} + \Delta_{0\mathbf{q}}\right) + \frac{\left(\phi_{\rm A}\phi_{\rm B} D_{\mathbf{q}} T_{\mathbf{q}} - \phi_{\rm A}\phi_{\rm B} D_{\mathbf{q}} T_{\mathbf{q}}\right)^2}{S^{\rm tot}_{\mathbf{q}} T^2_{\mathbf{q}}} \\ &= \phi_{\rm A}\phi_{\rm B} S_{\mathbf{q}} \qquad \text{(C.1)} \end{aligned}$$

where

$$S_{\mathbf{q}} = T_{\mathbf{q}} + \Delta_{0\mathbf{q}} = \overline{\langle \rho_{\mathbf{q}} \rho_{-\mathbf{q}} \rangle_0}^0$$

is the bare single chain structure factor, calculated in the absence of excluded volume interactions. The equation (C.1) is thus identical to equation (28) of reference [23].

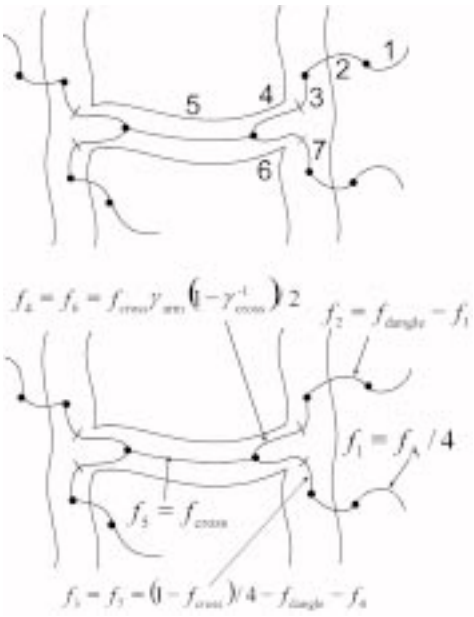

Fig. 8. Schematic diagram of an H-polymer which has a partially retracted crossbar ($\gamma_{\rm cross} > 1$) after a stretch. The polymer is divided into various sections of chain in different parts of the polymer tube. The end of each arm has escaped from the tube by star-like breathing modes. Also shown is the fraction f of the total molecular weight in each section of the polymer.

Appendix D: Calculation of one of the H-polymer structure factors

In this Appendix, we show (as an example) the calculation of the most important terms in one of the structure factors in the H-shaped polymer, $T^{\rm AB}_{0\mathbf{q}}$. Figure 8 is a schematic diagram of an H-polymer which has a partially retracted crossbar ($\gamma_{\rm cross} > 1$) after a stretch. The polymer is divided into various sections of chain in different parts of the polymer tube. The end of each arm has escaped from the tube by star-like breathing modes, and is isotropically distributed. Also shown is the fraction f of the total molecular weight in each section of the polymer.

To calculate $T^{\rm AB}_{0\mathbf{q}}$ we need to calculate correlation functions of the form $\overline{\langle \rho^{\rm I}_{\mathbf{q}} \rho^{\rm J}_{-\mathbf{q}} \rangle_0 - \langle \rho^{\rm I}_{\mathbf{q}} \rangle_0 \langle \rho^{\rm J}_{-\mathbf{q}} \rangle_0}^0$ between the labelled "A" sections of the polymer (Sect. 1 in the figure) and the unlabelled "B" sections of the polymer (Sects. 2, 3, 4, ...). We then find:

$$T^{\rm AB}_{0\mathbf{q}} = 4\left(T^{12}_{0\mathbf{q}} + T^{13}_{0\mathbf{q}} + T^{14}_{0\mathbf{q}} + T^{15}_{0\mathbf{q}} + T^{16}_{0\mathbf{q}} + T^{17}_{0\mathbf{q}} + ...\right). \qquad \text{(D.1)}$$

We could, in principle, include all of the "B" sections of the chain but, within the Warner-Edwards model, the contribution to of two chain segments to $T^{\rm AB}_{0\mathbf{q}}$ decays rapidly with increasing separation along the tube. It is excessive to include even the 1-5, 1-6 and 1-7 terms in the above expansion.

We do not explicitly solve the Warner-Edwards model for the branched polymer with dangling ends. Instead, we make sensible modifications to the results of (21, 22, 23)

$$T_{0\mathbf{q}}^{13}+T_{0\mathbf{q}}^{14}=\int_{f_2}^{f_1+f_2}\mathrm{d}x_1\int_0^{f_3+f_4}\mathrm{d}x_2\exp\left[-\sum_\mu\left(\begin{array}{c}Q_\mu^2\lambda_\mu^2\left\{\frac{x_2}{\gamma_{\rm arm}}-\zeta^2\left(1-\exp\left(-\frac{x_2}{\gamma_{\rm arm}\zeta^2}\right)\right)\right\}\\ +Q_\mu^2\zeta^2\left(1-\exp\left(-\frac{x_2}{\zeta^2}\right)\right)+Q_\mu^2x_1\end{array}\right)\right]$$
$$-\exp\left[-\sum_\mu\left(\begin{array}{c}Q_\mu^2\lambda_\mu^2\left\{\frac{x_2}{\gamma_{\rm arm}}-\zeta^2\left(1-\exp\left(-\frac{x_2}{\gamma_{\rm arm}\zeta^2}\right)\right)\right\}\\ +Q_\mu^2\zeta^2+Q_\mu^2x_1\end{array}\right)\right]. \tag{D.3}$$

$$T_{0\mathbf{q}}^{15}=\int_{f_2}^{f_1+f_2}\mathrm{d}x_1\int_{f_3+f_4}^{f_3+f_4+f_5}\mathrm{d}x_2\exp\left[-\sum_\mu\left(\begin{array}{c}Q_\mu^2\lambda_\mu^2\left\{\frac{x_2-f_3-f_4}{\gamma_{\rm cross}}+\frac{f_3+f_4}{\gamma_{\rm arm}}-\zeta^2\left(1-\exp\left(-\frac{x_2-f_3-f_4}{\gamma_{\rm cross}\zeta^2}-\frac{f_3+f_4}{\gamma_{\rm arm}}\right)\right)\right\}\\ +Q_\mu^2\zeta^2\left(1-\exp\left(-\frac{x_2}{\zeta^2}\right)\right)+Q_\mu^2x_1\end{array}\right)\right]$$
$$-\exp\left[-\sum_\mu\left(\begin{array}{c}Q_\mu^2\lambda_\mu^2\left\{\frac{x_2-f_3-f_4}{\gamma_{\rm cross}}+\frac{f_3+f_4}{\gamma_{\rm arm}}-\zeta^2\left(1-\exp\left(-\frac{x_2-f_3-f_4}{\gamma_{\rm cross}\zeta^2}-\frac{f_3+f_4}{\gamma_{\rm arm}}\right)\right)\right\}\\ +Q_\mu^2\zeta^2+Q_\mu^2x_1\end{array}\right)\right]. \tag{D.4}$$

$$T_{0\mathbf{q}}^{16}=\int_{f_2}^{f_1+f_2}\mathrm{d}x_1\int_{f_3+f_4}^{2f_4+f_3}\mathrm{d}x_2\exp\left[-\sum_\mu\left(\begin{array}{c}Q_\mu^2\lambda_\mu^2\left\{\frac{2f_3+2f_4-x_2}{\gamma_{\rm arm}}-\zeta^2\left(1-\exp\left(-\frac{2f_3+2f_4-x_2}{\gamma_{\rm arm}}\right)\right)\right\}\\ +Q_\mu^2\zeta^2\left(1-\exp\left(-\frac{x_2}{\zeta^2}\right)\right)+Q_\mu^2x_1\end{array}\right)\right]$$
$$-\exp\left[-\sum_\mu\left(\begin{array}{c}Q_\mu^2\lambda_\mu^2\left\{\frac{2f_3+2f_4-x_2}{\gamma_{\rm arm}}-\zeta^2\left(1-\exp\left(-\frac{2f_3+2f_4-x_2}{\gamma_{\rm arm}}\right)\right)\right\}\\ +Q_\mu^2\zeta^2+Q_\mu^2x_1\end{array}\right)\right]. \tag{D.5}$$

$$T_{0\mathbf{q}}^{17}=\int_{f_2}^{f_1+f_2}\mathrm{d}x_1\int_{f_3+2f_4}^{2f_4+2f_3}\mathrm{d}x_2\exp\left[-\sum_\mu\left(\begin{array}{c}Q_\mu^2\lambda_\mu^2\left\{\frac{x_2-2f_4}{\gamma_{\rm arm}}-\zeta^2\left(1-\exp\left(-\frac{x_2-2f_4}{\gamma_{\rm arm}}\right)\right)\right\}\\ +Q_\mu^2\zeta^2\left(1-\exp\left(-\frac{x_2}{\zeta^2}\right)\right)+Q_\mu^2x_1\end{array}\right)\right]$$
$$-\exp\left[-\sum_\mu\left(\begin{array}{c}Q_\mu^2\lambda_\mu^2\left\{\frac{x_2-2f_4}{\gamma_{\rm arm}}-\zeta^2\left(1-\exp\left(-\frac{x_2-2f_4}{\gamma_{\rm arm}}\right)\right)\right\}\\ +Q_\mu^2\zeta^2+Q_\mu^2x_1\end{array}\right)\right]. \tag{D.6}$$

based on the separation of these formulae into contributions from the tube mean path (which is well defined) and fluctuations within the tube, which we take to be isotropic. In this process, it is helpful to think of terms derived from $\overline{\left\langle\rho_{\mathbf{q}}^{\rm I}\rho_{-\mathbf{q}}^{\rm J}\right\rangle_0}^0$ as being equivalent to averaged contributions from the same chain in the same tube *at the same time*, and $\overline{\left\langle\rho_{\mathbf{q}}^{\rm I}\right\rangle_0\left\langle\rho_{-\mathbf{q}}^{\rm J}\right\rangle_0}^0$ as being equivalent to averaged contributions from the same chain in the same tube *at well separated times* (*i.e.* times separated enough for the annealed variables such as dangling end orientation to relax).

Given this picture, we write the correlation functions as follows. $T_{0\mathbf{q}}^{12}$ involves two chain sections on the same (isotropic) dangling end, with a "fixed" end that can still fluctuate in position by a tube diameter's width;

$$T_{0\mathbf{q}}^{12}=\int_{f_2}^{f_1+f_2}\mathrm{d}x_1\int_0^{f_2}\mathrm{d}x_2\exp\left[-\sum_\mu Q_\mu^2\left|x_1-x_2\right|\right]$$
$$-\exp\left[-\sum_\mu Q_\mu^2\left(x_1+x_2+\zeta^2\right)\right] \tag{D.2}$$

$T_{0\mathbf{q}}^{13}$ and $T_{0\mathbf{q}}^{14}$ involve correlations between sections in a tube with stretch factor $\gamma_{\rm arm}$ and a section on the dangling end;

see equation (D.3) above.

The expression for $T_{0\mathbf{q}}^{15}$ needs to include the change in stretch factor to $\gamma_{\rm cross}$ at the branch point.

see equation (D.4) above.

The expressions for $T_{0\mathbf{q}}^{16}$ and $T_{0\mathbf{q}}^{17}$ need to include the folding back of the chain on itself at the branch point.

see equations (D.5, D.6) above.

References

1. J.S. Higgins, H. Benoit, *Neutron Scattering of Polymers* (Oxford Clarendon Press, 1995).
2. S.F. Edwards, Proc. Phys. Soc. (London) **88**, 265 (1966).
3. P.G. de Gennes, J. Phys. France **31**, 235-238 (1970).
4. S.F. Edwards, Proc. Phys. Soc. **92**, 9 (1967).
5. R.T. Deam, S.F. Edwards, Phil. Trans. R. Soc. A **280**, 317 (1976).
6. S.F. Edwards, Polymer **9**, 140 (1977).
7. M. Warner, S.F. Edwards, J. Phys. A **11**, 1649-1655 (1978).
8. E. Straube, V. Urban, W. Pyckhout-Hintzen, D. Richter, C.J. Glinka, Phys. Rev. Lett. **74**, 4464-4467 (1995).
9. S. Westermann, V. Urban, W. Pyckhout-Hintzen, D. Richter, E. Straube, Macromolecules **29**, 6165-6174 (1996).
10. E. Straube, V. Urban, W. Pyckhout-Hintzen, D. Richter, Macromolecules **27**, 7681-7688 (1994).
11. M. Doi, S.F. Edwards, *The Theory of Polymer Dynamics* (Oxford Clarendon Press, 1986), Sect. 7.5.3.
12. T.C.B. McLeish, J. Allgaier, D.K. Bick, G. Bishko, P. Biswas, R. Blackwell, B. Blottière, N. Clarke, B. Gibbs, D.J. Groves, A. Hakiki, R.K. Heenan, J.M. Johnson, R. Kant, D.J. Read, R.N. Young, Macromolecules **32**, 6734-6758 (1999).
13. M. Doi, S.F. Edwards, J. Chem. Soc., Faraday Trans. 2 **74**, 1789 (1978).
14. M. Doi, S.F. Edwards, J. Chem. Soc., Faraday Trans. 2 **74**, 1802 (1978).
15. M. Doi, S.F. Edwards, J. Chem. Soc., Faraday Trans. 2 **74**, 1818 (1978).
16. M. Doi, S.F. Edwards, J. Chem. Soc., Faraday Trans. 2 **75**, 38 (1979).
17. T.C.B. McLeish, Macromolecules **21**, 1062 (1988).
18. T.C.B. McLeish, Polym. Commun. **30**, 4 (1989).
19. M.G. Brereton, T.A. Vilgis, J. Phys. I France **2**, 581 (1992).
20. D.J. Read, M.G. Brereton, T.C.B. McLeish, J. Phys. II France **5**, 1679-1705 (1995).
21. F. Boué, K. Osaki, R.C. Ball, J. Polym. Sci. (Physics) **23**, 833-844 (1985).
22. R.C. Ball, T.C.B McLeish, Macromolecules **22**, 1911 (1989).
23. D.J. Read, T.C.B. McLeish, Macromolecules **30**, 6376-6384 (1997).
24. S.T. Milner, T.C.B. McLeish, Phys. Rev. Lett. **8**, 725-728 (1998).
25. D.J. Read, T.C.B McLeish, Phys. Rev. Lett. **80**, 5450 (1998).
26. D.J. Read, T.C.B McLeish, Phys. Rev. Lett. **79**, 87 (1997).
27. D.J. Read, Macromolecules **31**, 899-911 (1998).
28. F. Boué, M. Nierlich, G. Jannink, R.C. Ball, J. Phys. France, **43**, 137-148 (1982); J. Phys. Lett. France **43**, L-585 (1982); J. Phys. Lett. France **43**, L-593 (1982).
29. S.V. Panyukov, Y. Rabin, Macromolecules **29**, 7960 (1996).
30. C. Hayes, L. Bokobza, F. Boué, E. Mendes, L. Monnerie, Macromolecules **29**, 5036-5041 (1996).
31. S.V. Panyukov, JETP **75**, 347-352 (1992).
32. C. Rouf, J. Bastide, J. Pujol, F. Schosseler, J. Munch, Phys. Rev. Lett. **73**, 830-833 (1994).
33. A. Ramzi, F. Zielinski, J. Bastide, F. Boué, Macromolecules **28**, 3570 (1995).
34. M. Rubenstein, S. Panyukov, Macromolecules **30**, 8036-8044 (1997).
35. T. Ohta, K. Kawasaki, Macromolecules **19**, 2621 (1986).
36. G.H. Fredrickson, S.T. Milner, L. Leibler, Macromolecules **25**, 6341-6354 (1992).